

**AN INVESTIGATION OF MECHANICAL PROPERTIES OF  
6 SERIES ALUMINIUM ALLOYS AFTER  
THIXOFORMING PROCESS**

*A Thesis*

*Submitted in partial fulfillment of the  
requirement for award of the degree*

**MASTER OF ENGINEERING  
IN  
PRODUCTION AND INDUSTRIAL ENGINEERING**

*Submitted by:*

**Gurpinder Singh**

**Roll No. 820982001**

Under the Guidance of

**Dr. V.P Agarwal**

Visiting Professor

Thapar University,

Patiala



**DEPARTMENT OF MECHANICAL ENGINEERING**

THAPAR UNIVERSITY

PATIALA-147004, INDIA

DECEMBER- 2012

## DECLARATION

This is to certify that the thesis entitled "AN INVESTIGATION OF MECHANICAL PROPERTIES OF 6-SERIES ALUMINIUM ALLOYS AFTER THIXOFORMING PROCESS." is an authentic record of my study carried out as requirements for the award of the degree of **Master of Engineering in Mechanical (Production and Industrial) Engineering** to **Thapar University, Patiala**, under the guidance of **Dr. V.P.AGRAWAL, Visiting Professor, Department of Mechanical Engineering, Thapar University, Patiala** during **Jan 2012 to Dec 2012**. The matter embodied in this thesis has not been submitted in part or full to other university or institute for the award of any degree.



**(GURPINDER SINGH)**

This is to certify that the above declaration made by the student concerned is correct to the best of my knowledge and belief.



**(Dr. V.P.AGRAWAL)**  
Visiting Professor,  
Thapar University,  
Patiala- 147004.

*Countersigned by:*



**(Dr. AJAY BATISH)**  
Professor and Head,  
Department of Mechanical Engineering,  
Thapar University, Patiala-147004.



**(Dr. S.K. MOHAPATRA)**  
Dean of Academic Affairs,  
Thapar University,  
Patiala-147004.

## ACKNOWLEDGEMENT

I am highly grateful to Ajay Batish, Professor and Head (MED) and Dr. S.K. Mohapatra, Dean of Academic Affairs, Thapar University, Patiala for providing this opportunity to carry out the Thesis work.

I would also like to express a deep sense of gratitude and thank profusely to my thesis guide Dr. V.P. Agrawal for his sincere and invaluable guidance, suggestions and attitude which inspired me to submit this thesis in the present form.

I would highly thank to Valco Industries Ltd. which provided me set up for this experiment and Mr. Chaturvedi and all the Valco staff.

I am highly thankful to Mr. Sukhbir and Mr. Narinder and all the workshop staff who helped me in various aspects of my research.

I would like to thank my friends Kashish, Aman, Gagan and Ashok for their cooperation.

I am also thankful to all faculty members of Mechanical Department, TU, Patiala for their intellectual report. My special thanks are due to my family members and friends who constantly encouraged me to complete this study.

  
(GURPINDER SINGH)

## **ABSTRACT**

Thixoforming process is new technique for manufacturing complicated and net shape components through which high strength materials can be formed easily. Thixoforming process consists of an injection into the component die of material at semisolid state. In order to get the thixotropic behavior of the material (viscosity which decreases with increase of shear stress and time), In this study 6-series Al alloys has been extruded by thixoextrusion process (Temperature ranging from 550 to 590°C) and its mechanical properties was compared. In this Thixoforming process by apply the advantage of semi solid processing, the applied pressure of extrusion is decrease and the desired mechanical properties were improved as comparison to conventional extrusion process of 6-series Al alloy under T6 condition. For example: Tensile and yield strength of samples of Thixoforming product improve and sufficiently agree with same expected properties of 6-series Al alloys and hardness, elongation is increase with Thixoforming process.

## TABLE OF CONTENTS

S.No.	Topic	Page No.
	<b>DECLARATION</b>	i
	<b>ACKNOWLEDGEMENTS</b>	ii
	<b>ABSTRACT</b>	iii
	<b>ABBREVIATIONS</b>	ix
	<b>NOTATIONS</b>	xi
	<b>LIST OF FIGURES</b>	xii
	<b>LIST OF TABLES</b>	xiii
	<b>CHAPTER-1</b>	
	<b>INTRODUCTION</b>	
1.1	Introduction	1
1.2	Thixoforming Process	1
1.3	History of Extrusion and Thixoextrusion Process	2
1.4	Working Principle of Extrusion Process	4
1.5	Extrusion Process Parameter	6
1.6	Organization of Thesis	6
	<b>CHAPTER-2</b>	
	<b>LITERATURE REVIEW</b>	
2.1	Introduction	8
2.2	Literature Survey	8
2.3	Gaps in Literature	19
2.4	Proposed Work	19
	<b>CHAPTER-3</b>	
	<b>DETAILED DESCRIPTION OF EXTRUSION PROCESS</b>	
3.1	Extrusion Method	21
3.2	Thixoforming Process	21
3.2.1	Advantage of Thixoforming Process	21
3.2.2	Limitation of the Thixoforming Process	22
3.3	Classification of Extrusion Process	23
3.3.1	Direct Extrusion	23
3.3.2	Indirect Extrusion	24
3.3.3	Forward and Backward Extrusion	24
3.3.4	Cold Extrusion	24
3.3.5	Impact Extrusion	25
3.3.6	Hot Extrusion	25
3.4	Extrusion Equipment	25
3.5	Advantage of Extrusion Process	26
3.6	Limitation of Extrusion Process	27

	<b>CHAPTER 4</b>	
	<b>MATERIAL AND EQUIPMENTS SPECIFICATIONS</b>	
4.1	Material Selection	28
4.1.1	Heat Treatable Aluminium Alloys	30
4.1.2	Non Heat Treatable Aluminium Alloys	31
4.2	Material Used	31
4.2.1	6063 Aluminium Alloy	32
4.2.2	6082 Aluminium Alloy	32
4.3	Equipments Used	33
4.3.1	Melting Furnace	33
4.3.2	Hot top - Billet Casting	34
4.3.3	Blade Heater	34
4.3.4	Extrusion Press	35
4.3.5	Hydraulic Stretcher	36
4.3.6	Aging Heater	36
4.3.7	Universal Testing Machine	37
4.3.8	Rockwell cum Brinell hardness testing machine	38
4.3.9	Scanning Electron Microscope Machine	39
4.3.10	X-RAY Diffraction Machine	39
	<b>CHAPTER 5</b>	
	<b>METHODOLOGY AND PROCEDURE</b>	
5.1	Procedure	40
5.1.1	Recrystallization and Partial Melting	43
5.2	Design of Extrusion Process	44
5.3	Aging Process	45
5.4	Output Parameters	46
5.4.1	Tensile strength ( $R_m$ )	46
5.4.2	Yield Strength	46
5.4.3	Proof strength ( $R_p$ )	46
	<b>CHAPTER 6</b>	
	<b>RESULT AND ANALYSIS OF UTS</b>	
6.1	Introduction	47
6.2	Analysis of UTS	47
6.2.1	Preparation of test piece	47
6.2.2	Test temperature	49
6.2.3	Test Procedure	49
6.2.3.1	Determination of Original Cross Section Area ( $S_o$ )	49
6.2.3.2	Marking the Original Gauge Length( $L_o$ )	49
6.2.3.3	Gripping of Test Piece	49
6.2.3.4	Loading of the Test Piece	49
6.2.3.5	Determination of Tensile Strength ( $R_m$ )	49
6.2.3.6	Determination of Upper yield Strength( $R_{eH}$ )	49
6.2.3.7	Determination of lower Yield Strength ( $R_{eL}$ )	49
6.2.3.8	Determination of proof strength ( $R_t$ )	50
6.2.3.9	Determination of percentage elongation after fracture(a)	50
6.2.3.10	Determination of Percentage Reduction of Area ( $Z$ )	50

6.3	Results for UTS	50
6.3.1	Results of tensile test of 6063 Aluminium Alloy	50
6.3.2	Results of tensile test of 6082 Aluminium Alloy	55
	<b>CHAPTER 7</b>	
	<b>RESULTS &amp; ANALYSIS OF HARDNESS</b>	
7.1	Introduction	61
7.2	Rockwell Test	61
7.2.1	Designation of Rockwell and Rockwell superficial Hardness	61
7.2.2	Apparatus	62
7.2.2.1	Testing Machine	62
7.2.3	Test conditions	62
7.2.3.1	Hardness Scale	62
7.2.4	Test Piece	62
7.2.4.1	Surface	62
7.2.4.2	Surface Preparation	62
7.2.4.3	Thickness	62
7.2.5	Spacing of indentation	62
7.2.6	Anvil	63
7.2.7	Test temperature	63
7.2.8	Test Procedure	63
7.2.9	Result and Analysis of Rockwell Hardness	63
7.3	Brinell Hardness Test	64
7.3.1	Designation of Brinell hardness	64
7.3.2	Apparatus	65
7.3.2.1	Testing Machine	65
7.3.3	Test Condition	65
7.3.3.1	Force- Diameter ratio	65
7.3.3.2	Test Force	65
7.3.3.3	Indenter	65
7.3.4	Test Piece	65
7.3.4.1	Surface	65
7.3.4.2	Surface Preparation	66
7.3.4.3	Thickness	66
7.3.5	Spacing of Indentation	66
7.3.6	Anvil	66
7.3.7	Test temperature	66
7.3.8	Test Procedures	66
7.3.9	Results and Analysis of Brinell Hardness	67
7.4	Micro Hardness Tester	68
	<b>CHAPTER-8</b>	
	<b>SEM AND XRD ANALYSIS</b>	

8.1	Introduction	70
8.2	Microstructure Analysis	70
8.2.1	Repairing Samples for SEM	70
8.3	XRD analysis	73
8.3.1	XRD Analysis of Al-6082 alloy at temperature of 548 °C	73
8.3.2	XRD Analysis of Al-6063 alloy at temperature of 545 °C	73
8.3.3	XRD Analysis of Al-6063 alloy at temperature of 560 °C	74
8.3.4	XRD Analysis of Al-6082 alloy at temperature of 585 °C	75
	<b>CHAPTER-9</b>	
	<b>RESULTS, CONCLUSIONS AND RECOMMENDATIONS</b>	
9.1	Introduction	76
9.2	Results of UTS	76
9.2.1	Ultimate and Proof Stress	77
9.2.2	Elongation of Material	77
9.2.3	Reduction in Area	77
9.3	Result of Hardness	77
9.3.1	Rockwell Hardness	78
9.3.2	Brinell Hardness	78
9.3.3	Micro Hardness	78
9.4	Conclusions	78
9.5	Recommendation for Future Work	79

## LIST OF FIGURES

<b>Figure No.</b>	<b>Caption</b>	<b>Page No.</b>
1.1	Extrusion Process set	5
1.2	Pressure-Displacement Curve	5
3.1	Mechanism of Direct Extrusion	23
3.2	Mechanism of Indirect Extrusion	24
4.1	Melting Furnace	33
4.2	Hot top Billet Casting System	34
4.3	Blade Heater	35
4.4	Horizontal Extrusion Press	35
4.5	Hydraulic Stretcher	36
4.6	Ultimate Tensile machine	37
4.7	Rockwell Hardness Machine	39
5.1	Flow chart of Procedure	42
5.2	Recrystallization And Partial melting	43
5.3	Design of Extrusion Process	44
5.4	Aging Process	45
5.5	Output Parameters	46
6.1	Dimension UTM Sample	48
6.2	UTM Samples	48
6.3	UTS of 6063 Al alloy at 545°C [Trail 1]	51
6.4	UTS of 6063 Al alloy at 545°C [Trail 2]	51
6.5	UTS of 6063 Al alloy at 545°C [Trail 3]	52
6.6	UTS of 6063 Al alloy at 545°C [Trail 4]	52
6.7	UTS of 6063 Al alloy at 560°C [Trail 1]	53
6.8	UTS of 6063 Al alloy at 560°C [Trail 2]	54
6.9	UTS of 6063 Al alloy at 560°C [Trail 3]	54
6.10	UTS of 6063 Al alloy at 560°C [Trail 4]	54
6.11	UTS of 6082 Al alloy at 548°C [Trail 1]	56
6.12	UTS of 6082 Al alloy at 548°C [Trail 2]	56
6.13	UTS of 6082 Al alloy at 548°C [Trail 3]	57
6.14	UTS of 6082 Al alloy at 548°C [Trail 4]	57
6.15	UTS of 6082 Al alloy at 585°C [Trail 1]	58
6.16	UTS of 6082 Al alloy at 585°C [Trail 2]	59
6.17	UTS of 6082 Al alloy at 585°C [Trail 3]	59
6.18	UTS of 6082 Al alloy at 585°C [Trail 4]	60
6.19	UTM Samples after break	60

7.1 (a)	Indentation on Al-6063 at 545°C	68
7.1 (b)	Indentation on Al-6063 at 560 °C	68
7.2 (a)	Indentation on Al-6082 at 548 °C	69
7.2 (b)	Indentation on Al-6082 at 585°C	69
8.1	SEM Samples	70
8.2	SEM Analysis of Al-6082 at temperature 548°C	71
8.3	SEM Analysis of Al-6082 at temperature 585°C	71
8.4	SEM Analysis of Al-6063 at temperature 545°C	71
8.5	SEM Analysis of Al-6063 at temperature 560°C	72
8.6	Al-6063 alloy at temperature 545°C	73
8.7	Al-6063 alloy at temperature 560°C	74
8.8	Al-6082 alloy at temperature 548°C	74
8.9	Al-6082 alloy at temperature 585°C	75

## **ABBREVIATIONS**

<b>UTS</b>	Ultimate Tensile Strength
<b>UTM</b>	Ultimate Testing Machine
<b>XRD</b>	X- Ray Diffraction
<b>RAP</b>	Recrystallization and Partial melting
<b>SEM</b>	Scanning Electron Microscope

## NOTATIONS

$R_m$	Tensile Strength
$R_p$	Proof Stress
$R_{eH}$	Upper Yield Strength
$R_{eL}$	Lower Yield Strength
$S_o$	Original Cross section Area
$S_u$	Minimum Cross section Area after fracture
$L_o$	Original Gauge Length
$L_u$	Final Gauge Length
$F_m$	Maximum Force
$A$	Percentage Elongation after fracture
$Z$	Percentage Reduction of Area

### INTRODUCTION

#### 1.1 Introduction

Extrusion is defined as a process by which a block of metal is reduced in cross-section by forcing it to flow through a die under high pressure. Main advantage of extrusion is that high compressive stresses are set up in the billet due to its reaction with a container and die. These stresses are effective in reducing the cracking of materials during primary breakdown from the billet. Due to this, large reduction are possible in also the difficult metal can be extruded for e.g. stainless steel , Nickel based alloy and other high temperature materials. Extrusion can be used both for hot and cold working. Also bars, hollow tube and shape of irregular cross-section can be extruded. Extrusion could be considered as adaption of closed die forging, the difference being that in a forging, the main body of the metal is the product and flash is cut away and discarded, in extrusion the flash in the product and the slug remaining in the die is not used. In simple, it is defined as the process of shaping materials such as aluminum, by forcing it to flow through a shaped opening in a die. Extruded material emerges as an elongated piece with the same profile as the die opening. The most important factor to remember in the extrusion process is temperature. Temperature is most critical because it gives aluminum desired characteristics such as hardness and finish.

#### 1.2 Thixoforming Process

Thixoforming process consists of an injection into the component die of material at semisolid state. In order to get the thixotropic behavior of the material (viscosity which decreases with increase of shear stress and time), its structure before injection has to be composed of solid globular dendrites dispersed in liquid eutectic fraction (rheocast structure). Therefore the material has to be undergone at a preliminary procedure for obtaining billets having the right structure suitable for Thixoforming process. More methods are available for reaching this structure: electromagnetic stirring, mechanical stirring, passive stirring, grain refinement. Electromagnetic steering is the most used for aluminum alloys. During solidification, the steering breaks the tree dendrites which solidify with spheroidal shape [5].

### **1.3 History of Extrusion and Thixoextrusion Process**

The earliest investigations into the principles of the extrusion were done by a hydraulic engineer named Joseph Brannah. He described a press for making lead pipes of all dimensions and lengths without connecting joints and received a patent for his ideas in 1797. There were no immediate developments in his ideas and the earlier methods for making pipes were still being used. It was not until 1820 That Thomas Burr, a Shrewsbury plumber, constructed a press operated by hydraulic power for the manufacture of lead pipes by "squirting", (the original term describing the extrusion process).

A modified press taken from burr's ideas was made by J. and C. Hanson in 1837. This improved model fixed the die in the bottom of the container eliminating the awkwardness of the previous charging method. This improvement was achieved by incorporating a hole in the upper part of the container wall which was sealed by a plunger at the beginning of the working stroke. The new design featured a means of centering the die. This feature introduced improved concentricity in the pipe and retained in principle for developing future theories.

By the middle of the 1800's the extrusion process had become firmly established. New developments came about from the interest in the production of Tin-lined pipes to overcome the dangers of corrosion which occurred when lead pipes were used to convey waters and liquids. In 1863, Shaw used a press which precast hollow billets of lead with inner cast sleeves of Tin. There were difficulties in arriving at the correct shape of the sleeve to give a uniform lining of Tin in the pipe. We now understand these complications by knowing the complexities in the direct method of the extrusion which was solely used at that time.

Up until this time, the applications of the extrusion principle were concentrated mainly in industry for developing more advanced tools for production. But, in the scientific world, Tresca opened these theories for analysis in 1864.

The next stage in the evolution of the pipe press in industry was brought about by the introduction of the indirect or inverted method of extrusion by J. and W. Weems in 1870. This method alters the course of deformation occurring in the billet. The metal remained undisturbed by avoiding a displacement of the billet and the walls of the container. This made it possible to produce a more even coating of tin in the pipe.

Although the development of the extrusion process was most directly related to the lead pipe industry, a noteworthy advancement was patented by Cunningham in 1873. He invented a

device which, by extrusion, curved lead pipes for use as siphons, bends or traps. Bend presses continued to be in common use through the twentieth century.

Rapid expansion in the electrical industry about this time brought about the need for a protective envelope for cables which would help prevent mechanical damage and be impervious to water. Lead was used in 1845 by Wheatstone and Cooke in the form of a strip which surrounded the conductor and soldered along the overlapping edges. This was achieved by threading cable through 50-foot lengths of lead pipe and joined at the ends by soldering, leaving the cable only loosely encased. Seeing opportunity, Borel of France and Wesslau of Germany devised methods to extrude lead sheathing directly onto the cable in 1879. Although it worked successfully, it had a disadvantage in that a continuous length of cable with sheathing could not be cut to allow a fresh billet to be inserted.

Two years later, Huber in Germany devised a press similar in method which defeated the problems of Borel and Wesslouts design. His press enable long lengths of cable to be sheathed without the necessity for joints. Because, the consecutive charges of lead were adapted into the containers at the end of each extrusion stroke. This came to be known as the horizontal press. Concurrently with its development, came about the evolution of the vertical cable press in 1880by Eaton from the United States.

The advanced state to which the extrusion was applied to the lead industry led attention towards the possible utilization of other metal which possessed better mechanical properties. But, the lead presses were unsuitable for the job. It was found that even the metal most susceptible to hot working did not become sufficiently plastic to undergo the heavy deformation involved in an extrusion. It was due to Alexander Dick that all obstacles were removed from the situation. It was the inventive genius of this man which laid the foundations for the modern hot extrusion process. He patented his ideas in 1894 and was followed by others.

Up until world war one, the extrusion process was considered simple in principle due to limited knowledge of designers of hydraulic machinery at that time. The increased use of brass bars for ammunition components broadened the scope for a metallurgical investigation at Woolwich, U.K.. This investigation leads to a better plastic flow of metals during an extrusion. By opening this field, experiments with plasticine and wax provide reasons for debate. The behavior of wax under extrusion conditions could not be readily translated into a high temperature practice with metals, So the Woolwich investigators made small scale experiments with brass for modifying

the mode of flow during the extrusion. An apparatus was improvised to use under a vertical press and all parts were at a dull red heat and prone to collapse under high loads. To the investigators, these experiments were not without adventure and eventually the evidence needed was giving new light to the process of the “inverted” extrusion which utilizes the advantages of a low working pressure with the complete avoidance of defects in their product.

Systematic research on the extrusion was noted in 1931 by Eisbein, Sachs, Seibel and Frangmeier. These analyses were based on the “Total Strain Theory” until the appearance of Hill's work in 1948 which utilized the “Slip-Line Theory”. Johnson later devised the upper-bound approach technique for the approximate analysis of the extrusion.

In 1953 Pearson Patented the process for producing lead tubes by extrusion. Thereafter, attention was focused on working with harder metal and alloys. The semi-empirical analysis technique using strain distribution measurements was developed by Thomsen and Frish which were later reviewed by Bishop in 1957, who added further contributions to its theory.

The early 1960's exemplified the application of the extrusion process in working with steel at elevated and room temperatures in industry. Nuclear energy industries extruded specially brittle metals such as titanium, and beryllium. Through progress, dedication of scientists and a great deal of effort, the extrusion process is now a well defined theory applicable to the most advanced areas in the field of mechanical engineering.

The potential for forming processes based upon semi-solid metal alloys was first recognized in the early 1970s. The microstructure of a suitable alloy comprises spheroidal particles of solid surrounded by liquid phase of a lower melting point, rather than the interlocking tree-like dendrites of conventionally cast alloy. It is this microstructure that gives the material its thixotropic properties, i.e. when sheared the material flows, but when allowed to stand, it thickens. Thixoforming is one member of a family of semi-solid forming processes and it possesses characteristics of both casting and forging. The non-dendritic feedstock necessary for thixoforming is usually produced using electromagnetic stirring in a continuous casting process [39].

#### **1.4 Working Principle of Extrusion Process**

For more than 60-years existence of extrusion technologies a wide variety of machine designs for their realization has appeared. Extrusion is short-time high-temperature process which is successfully applied both in food and feed mill industries. The operation principle of extruders

is determined by the technological essence of an extrusion process. Extrusion is a complex physico-chemical process which goes under the influence of mechanical force, moisture and high-temperature. The processed product is heated up due to the transformation of mechanical energy into heat which is escaped at overcoming an internal friction and plastic deformation of the product or due to external heating.

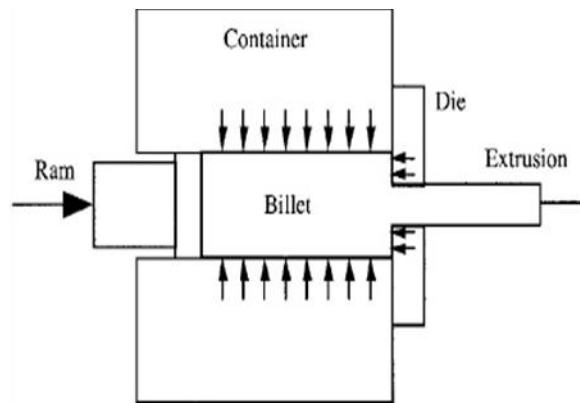


**Fig.1.1 Extrusion Process set [40]**

Figure 1.1 shows the principle of direct extrusion where the billet is placed in the container and pushed through the die by the ram pressure. Direct extrusion finds application in the manufacture of solid rods, bars, hollow tubes, and hollow and solid sections according to the design and shape of the die. In direct extrusion, the direction of metal flow will be in the same direction as ram travel. During this process, the billet slides relative to the walls of the container. The resulting frictional force increases the ram pressure considerably.

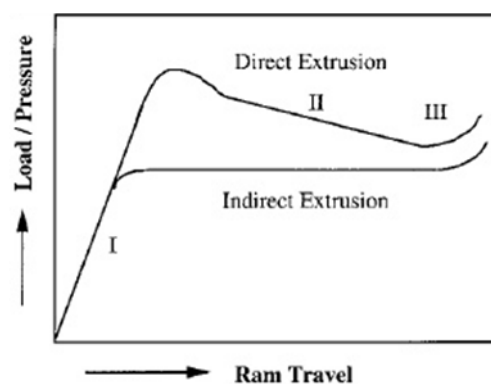


**Fig 1.2 Pressure-Displacement Curve [40]**

During direct extrusion, the load or pressure-displacement curve most commonly has the form shown in Fig. 1.2. Traditionally, the process has been described as having three distinct regions:

1. The billet is upset, and pressure rises rapidly to its peak value.

2. The pressure decreases, and what is termed “steady state” extrusion proceeds.
3. The pressure reaches its minimum value followed by a sharp rise as the “discard” is compacted.

### **1.5 Extrusion Process Parameter**

The changeable parameters of extrusion processing are raw material content, its nature and humidity. During extrusion changes of temperature, pressure, duration and intensity of the influence on raw material are possible. There are three basic extrusion techniques: cold forming, thermal processing and forming and so-called "hot" extrusion. Recently the method of "hot" extrusion which is carried out at high-rates, pressure and significant transition of mechanical power in thermal has become widespread.

### **1.6 Organization of Thesis**

**Chapter 1** cover brief Introduction to Extrusion and Thixoextrusion process, working principle of extrusion and Thixoextrusion.

**Chapter 2** presents an available literature of Thixoforming process. The available literature has been categorized in two board classification such as improvement of mechanical properties of material and improvement in microstructure of material. Summary of literature and gap in literature also discussed, objective and work plan also discussed.

**Chapter 3** presents the detail description of extrusion like classification, advantage, disadvantage and also describe the equipment used in experiment.

**Chapter 4** presents the introduction of working material (Aluminum alloy 6063, 6082), equipment specifications to be adopted also describe in brief.

**Chapter 5** presents the methodology and the procedure of experimental work in brief and also describe the introduction of mechanical strength of material like ultimate tensile strength, yield strength and proof strength..

**Chapter 6** presents the detail description of UTS test like preparation of sample, test condition, test procedure and also analysis the result of UTS.

**Chapter 7** presents the detail description of different hardness and describe preparation of sample, test condition, test procedure for these operations and also analysis the result of different hardness test.

**Chapter 8** presents the analysis and result of Scanning Electron Microscope and X-Ray Diffraction.

**Chapter 9** presents the analysis and result of ultimate tensile strength, elongation, reduction in area, different hardness and also describe the results, conclusion and recommendation from the experiment work.

**LITERATURE REVIEW****2.1 Introduction**

The potential for forming processes based upon semi-solid metal alloys was first recognized in the early 1970s. A lot of research has been carried out through the world for studying Thixoforming process on various alloys. The rapid progress in this field is clear from the number of published papers.

**2.2 Literature Survey**

**Dey S. et al. [1]** Fatigue lives at high peak stresses for peak-aged (T6) and over aged (T73) 7075 aluminum alloy were compared in the uncorroded and pre-corroded (pitted) states. Absolute fatigue lives of T73 samples were much higher than that of T6 in the virgin as well as pre-corroded condition, but the normalized life of T73 was less than that of T6, indicating an intrinsic crack initiation resistance in the former, borne out by fractography, which showed that fatigue cracks almost always initiated at pits for T73 but not for T6. The various crack initiation methodologies observed and the effect of pitting on fatigue lives in the two aging conditions are discussed.

**Xue Y. et al. [2]** The multistage fatigue model for high cycle fatigue of a cast aluminum alloy developed by McDowell et al. is modified to consider the structure–property relations for cyclic damage and fatigue life of a high strength aluminum alloy 7075-T651 for aircraft structural applications. The multistage model was developed as a physically-based framework to evaluate sensitivity of fatigue response to various micro structural features to support materials process design and component-specific tailoring of fatigue resistant materials. In this work, the model is first generalized to evaluate both the high cycle fatigue (HCF) and low cycle fatigue (LCF) regimes for multi-axial loading conditions, with appropriate modifications introduced for wrought materials. The particular micro structural features of relevance to fatigue in aluminum alloy 7075-T651 include micron -scale Fe-rich intermetallic particles and rolling textures. The model specifically addresses the role of local constrained cyclic micro plasticity at fractured inclusions in fatigue crack incubation and micro structurally small crack growth, including the effect of crystallographic orientation on crack tip displacement as the driving force. The model is able to predict lower and upper bounds of the fatigue life based on measured inclusion sizes.

**Yang Y. et al. [3]** The spatial distribution of shear bands was investigated in the rolled 7075 aluminum alloy through the thick-walled cylinder (TWC) technique with  $0^\circ$ ,  $90^\circ$  and  $45^\circ$  angles between the aluminum alloy cylinder axial direction and the rolling direction. Self-organization of multiple adiabatic shear bands was observed in different orientation specimens and investigated by using Schmid factor theories. The experimental results indicated obvious differences in the morphology and self-organization of shear bands for the specimens. At the initial stage, the spacing of the shear bands in the  $0^\circ$  specimen is smaller than in the other specimens. The nucleation of the shear bands in the  $90^\circ$  specimen is early. Due to the shielding effect, fast-developed shear bands block the development of the neighboring smaller shear bands in the  $90^\circ$  specimen. The spacing of the shear bands in the  $45^\circ$  specimen is much larger than in the other specimens under the similar effective strain. At the late stage, a large number of shear bands nucleate in the  $0^\circ$  specimen, and the spacing of the shear bands is small. The shear bands in the  $90^\circ$  specimen are well-developed with obvious shielding effect and the largest spacing. The  $45^\circ$  specimen has the maximum average nucleation rate of the shear bands. Owing to the close Schmid factors of the slip systems of the  $45^\circ$  specimen, the spacing of the shear bands in the  $45^\circ$  specimen is still larger than in the  $0^\circ$  specimen.

**Yang Y. et al. [4]** the self-organization behaviors of multiple adiabatic shear bands (ASBs) in the 7075 T73 aluminum alloy were investigated by means of the thick-walled cylinder (TWC) technique. Shear bands first nucleate at the inner boundary of the aluminum alloy tube and propagate along the maximum shear stress direction in the spiral trajectory. On the cross section of the specimen, shear bands distribute either in the clockwise or the anticlockwise direction. The number of ASBs in the clockwise direction is roughly twice that in the anticlockwise direction. However, the 7075 annealed alloy does not generate any shear band under the same experimental conditions. Numerical simulation with coupled thermo-mechanical analysis was carried out to investigate the evolution mechanism of adiabatic shear bands. Both uniform and non-uniform finite element models were created. The simulation results of the non-uniform model are in better agreement with those of the experiment. In the non-uniform case, the spacing between ASBs is larger than that of the uniform model, and most of the ASBs prefer to propagate in the clockwise direction. For the first time, two types of particles (second phase), hard particles and soft particles, are separately introduced into the metal matrix in the non-uniform model to simulate their effects on the self-organization of ASBs. The soft particles reduce the time required for ASBs nucleation. Stress collapse first occurs at the region where the soft particles are located and most of the ASBs pass through these soft particles. However, ASBs propagate along the paths that are adjacent to the hard

particles instead of passing through them. As experimental observations, there is no shear band nucleating in the annealed alloy in simulation. Under the same conditions, the energy barrier for the formation of ASBs in the annealed aluminum alloy is about 2.5 times larger than that in the T73 alloy, which means that the adiabatic shearing is less likely to nucleate in the annealed alloy. This is consistent with the experimental and numerical simulation results.

**Chayong S. et al. [5]** Heat treated condition (505MPa and 11% elongation) commercially extruded 7075 alloy (extrusion ratio of 16:1) has been used as a feedstock for thixoforming in order to investigate thixoformability of a high performance aluminium alloy. The microstructure in the semi-solid state consists of fine spheroidal solid grains surrounded by liquid. The results of thixoforming with one step, two-step and three-step induction heating regimes are presented. Typical defects in poorly thixoformed material (e.g. liquid segregation, impedance of flow by unrecrystallised grains and porosity) are shown alongside successfully thixoformed material (thixoforming temperature of between 615 and 618 °C with a three-step induction heating regime). The highest yield strength and elongation obtained for material thixoformed into a simple graphite die and heat treated to the T6 condition is 478MPa and 6.9% elongation. For thixoforming at 615 °C into a tool steel die heated to 250 °C, the highest yield strength and elongation obtained are 474MPa and 4.7% (ram velocity 2000 mm/s). These values (particularly for strength) are approaching those of 7075 in the wrought.

**Vaneetveld G. et al. [6]** Thixoforging is a type of semi-solid metal processing at high solid fraction ( $0.5 < f_s < 1$ ). 7075 aluminium alloy has been used as a feedstock for Thixoforging in order to investigate thixoformability of a high performance aluminium alloy at high solid fraction. Higher solid fraction of 7075 alloy is less sensitive to a drop in temperature, avoids metal splash at high speed, and allows laminar flow at high speed. Hot tool is used to slow down the solidification rate of the high solid fraction metal by decreasing thermal exchanges. To determine the best parameters to achieve maximum mechanical properties in Thixoforging of 7075 aluminum alloy, we need to consider the impact of some parameters such as tool temperature, shear rate. For this, we use extrusion tests with constant speed where these parameters are known. The result of this study is that each parameter has its level of impact on the Thixoforging: the temperature of the tool and the deformation rate shouldn't be high to avoid cracks. Thermal exchanges between the material flow and the tool have to be reduced to avoid high solidification rate.

**Atkinson H.V. et al. [7]** 7000 series aluminium alloys are currently machined from the wrought state with much waste. There is therefore a motivation to identify effective near net shaping routes. Semi-solid processing is one such potential route. It relies on the thixotropic behavior of alloys with non-dendritic spheroidal microstructures. In the semisolid state the material thins when sheared and will flow to fill the die. When worked material is reheated, it recrystallises and moving into the semi-solid state, the required spheroidal microstructure develops. Here we examine the early stages of spheroid formation in 7075 aluminium alloy reheated from the as-supplied T6 condition. This alloy is very resistant to recrystallisation in the solid state due to the presence of dispersoid particles pinning grain boundaries. There is a sudden increase in the appearance of spheroidal grains. There is a close association with the position of the first liquid to form. On reheating as-supplied material to around 580°C (fraction of liquid ~5%), a fully spheroidal microstructure can be obtained.

**Rogal L. et al. [8]** among various methods of material preparation before thixoforming, applied to obtain globular microstructure, like cold or hot deformation, Equal Channel Angular Pressing ECAP allows to obtain the correct microstructure after heating to the semi-solid range. In the present study 7075 aluminium alloy was cold pressed using ECAP method in order to obtain the appropriate semi-solid range microstructure. The bar of 7075 alloy annealed at 400°C of diameter of 30 mm, was cold pressed using ECAP at a pressure of 800 MPa. Samples had only a small cracks and the hardness of 95 HV5. The characteristic temperature of the thixo-process was determined using DSC at 615°C which is slightly higher than that used in the literature. A series of a gear shape samples were thixo-formed from the alloy after ECAP using modified high pressure die casting. The globular microstructure with the globule's size between 60µm -90µm was observed. The hardness was lower than after ECAP, close to 80 HV5. Additionally, T6 heat treatment was performed: super saturation from 460°C and ageing for the period of 12 hours at 120°C. Transmission Electron Microscopy TEM enabled identification of precipitates of size near 20 nm present in the alloy after the thixoforming and T6 treatment, responsible for a rise of hardness up to 150 HV5.

**Dong J. et al. [9]** The as-cast microstructures, the evolution of the microstructures during reheating and the mechanical properties of thixoformed products of 7075 aluminum alloy cast by liquidus semi-continuous casting (LSC) were studied in this paper. When the melt was held for 30 min at the temperature (638°C) closely near its liquidus temperature, then was cast semi-continuously, a microstructure of fine, uniform and net-globular grains was obtained, which was satisfactory for meeting the microstructural requirement of thixoforming. Decrease first

cooling and the casting velocity, and increase second cooling were propitious to the formation of the fine, uniform and net-globular grains. The formation of the net-globular grains was resulted from the increase in the number of crystal nuclei and the decrease in growth velocity of grains during LSC. The net-globular and rosette-shaped grains obtained by LSC became spheroids during reheating. The optimum microstructure was obtained when the reheating temperature was near 580°C and the holding time was 15-30 min, or the reheating temperature was near 600°C and the holding time was 5-15 min. It was very easy to thixoform when the ingots were reheated to 600°C for 15 min. The ultimate strength of thixoformed products was 357.9 and 468 MPa before and after T6 treatment, respectively.

**Davim J. et al. [10]** the purpose of this paper is to study the thermal and mechanical behavior in machining of aluminum alloys (Al7075-0) using PCD (polycrystalline diamond) and K10 (cemented carbide) tools and to make a comparison between the performances of both tools. The study was made using commercial finite element software. This software has a user friendly interface and can output several results including cutting forces, temperature, pressure, von Mises stress, maximum shear stress, plastic strain, and plastic strain rate which were the objectives of this study. By analyzing the simulations, it was concluded that the polycrystalline tool has a superior performance in terms of cutting and feed forces and temperature when compared to the cemented carbide tool.

**Yang Y. et al. [11]** the fracture behaviors of the 7075 aluminum alloy under two different dynamic loading conditions are investigated by means of a light-gas gun. The fracture surfaces obtained in the spall test are compared to the fracture surfaces obtained with a blunt projectile struck to the aluminum alloy plate. Optical and scanning electron microscopes are used in the investigation. For the plate-impact test, spall of the target was attributed to intergranular fracture caused by the tensile stress. The fracture behavior during projectile penetration is complex and consists of several fracture modes in addition to that the fracture is also of dynamic character. The penetration process of aluminum alloy target included: plugging stage, the micro cracks nucleation stage, and the final tensile fracture stage. Mixed intergranular brittle/ductile fracture was observed, and brittle fracture played a dominate role.

**Kilickap E. et al. [12]** this investigation presents the use of Taguchi and response surface methodologies for minimizing the burr height and the surface roughness in drilling Al-7075. The Taguchi method, a powerful tool to design optimization for quality, is used to find optimal

cutting parameters. Response surface methodology is useful for modeling and analyzing engineering problems. The purpose of this paper was to investigate the influence of cutting parameters, such as cutting speed and feed rate, and point angle on burr height and surface roughness produced when drilling Al-7075. A plan of experiments, based on L27 Taguchi design method, was performed drilling with cutting parameters in Al-7075. All tests were run without coolant at cutting speeds of 4, 12, and 20 m/min and feed rates of 0.1, 0.2, and 0.3 mm/rev and point angle of 90°, 118° and 135°. The orthogonal array, signal-to-noise ratio, and analysis of variance (ANOVA) were employed to investigate the optimal drilling parameters of Al-7075. From the analysis of means and ANOVA, the optimal combination levels and the significant drilling parameters on burr height and surface roughness were obtained. The optimization results showed that the combination of low cutting speed, low feed rate, and high point angle is necessary to minimize burr height. The best results of the surface roughness were obtained at lower cutting speed and feed rates while at higher point angle. The predicted values and measured values are quite close to each other; therefore, this result indicates that the developed models can be effectively used to predict the burr height and the surface roughness on drilling of Al-7075.

**Chavoshi S. et al. [13]** flank wear occurs on the relief face of the tool and the life of a tool used in a machining process depends upon the amount of flank wear; so predicting of flank wear is an important requirement for higher productivity and product quality. In the present work, the effects of feed, depth of cut and cutting speed on flank wear of tungsten carbide and polycrystalline diamond (PCD) inserts in CNC turning of 7075 AL alloy with 10 wt% SiC composite are studied; also artificial neural network (ANN) and co-active neuro fuzzy inference system (CANFIS) are used to predict the flank wear of tungsten carbide and PCD inserts. The feed, depth of cut and cutting speed are selected as the input variables and artificial neural network and co-active neuro fuzzy inference system model are designed with two output variables. The comparison between the results of the presented models shows that the artificial neural network with the average relative prediction error of 1.03% for flank wear values of tungsten carbide inserts and 1.7% for flank wear values of PCD inserts is more accurate and can be utilized effectively for the prediction of flank wear in CNC turning of 7075 AL alloy SiC composite. It is also found that the tungsten carbide insert flank wear can be predicted with less error than PCD flank wear insert using ANN. With Regard to the effect of the cutting parameters on the flank wear, it is found that the increase of the feed, depth of cut and cutting speed increases the flank wear. Also the feed and depth of cut are the most effective parameters on the flank wear and the cutting speed has lesser effect.

**Shen J. et al. [14]** Spray deposition is a new rapid solidification technique which produces bulk performs directly from the melt metals. A spray deposition process was used to develop several high-strength aluminium alloys based on their commercial chemical compositions. These alloys include 2024 alloy, 7075 alloy and 7075 alloy modified with 1.0% Fe and 1.0% Ni. The deposits possessed rapid solidification microstructure with grain size of about 20  $\mu\text{m}$  and a relative density of over 94%. The hardening phases of the materials in T4 or T6 conditions consisted of supersaturated solid solution, stable and unstable ageing precipitates and disperse phases. The formation of the fine distributed disperse phases was due to the addition of iron and nickel to the 7075 alloy. The spray-deposited materials exhibited substantial improvement in tensile strengths and maintained acceptable ductility when compared to the corresponding ingot metallurgy processed materials.

**Anderson N. et al. [15]** It is widely accepted that the yielding of materials can be modeled to a satisfactory degree of accuracy. However the hardening behavior is a topic that needs attention. Recent experiments explored the evolution of hardening of sheet metals with off-axis straining, raising much debate about the nature of the behavior. In light of these results this paper aims to characterize the hardening behavior observed due to pre-straining in the sheet rolling direction. Aluminum alloy 7075-O is used for the examination. Further to this, the adequacy of the Leacock (2006) yield criterion in representing this behavior is assessed. Using this representation the discrete yielding behavior of 7075-O is successfully modeled.

**Lee D. et al. [16]** study was on the creep behavior of 7075 Al alloys. The stress exponent value in static creep was 8.9 and in cyclic creep were 8.7. The exponent values were well above the power law regime. They decreased with increasing temperature. The values of activation energy obtained were 241  $\text{kJ mol}^{-1}$  in static creep and 265  $\text{kJ mol}^{-1}$  in cyclic creep. These values were both higher than that of Al lattice diffusion. The constant values of the Larson–Miller parameter in static and cyclic creep were 14 and 10.7. The constant, 10.7, and the high activation energy, 265  $\text{kJ mol}^{-1}$  may explain the effect of cyclic creep retardation occurring over the entire test regime. It was found from the SEM results that the fracture mode in 7075 Al alloys was transgranular. The Cr-dispersoid ( $\text{Al}_{18}\text{Cr}_2\text{Mg}_3$ ) distributed extend extensively across all the grains were responsible for a rapid increase in void formation, resulting in ductile failure. The rupture time is strongly dependent on the dispersoid size.

**Zhang K. et al. [17]** The presence of SiC particles may restrict crystal growth of primary phase during laser rapid solidification of an aluminum 7075 alloy. Under the condition of higher

volume fraction of larger particles, non-epitaxial grain development is favored in laser resolidified zone.

**Chang S. et al. [18]** There were two ways employed to experimentally determine the tube spin ability of the full-annealed and solution-treated AA 2024 and 7075 aluminum alloys. Tube spin ability was defined as the maximum thickness reduction before either fracture or buckling under the given roller geometry, feed rate, and the speed of the mandrel during the tube spinning of a metal. One was to reduce the thickness stepwise to the final thickness without failure the tube. The other was the one-path spinning with continuous reduction in wall thickness of perform from initial to the final thickness without buckling to determine the achieved maximum reduction. Using continuous reduction test, the determined macro-spin ability of full-annealed AA 2024 aluminum alloys is 75% and 7075 aluminum is 74%. Whereas, when examined by scanning electron microscope, the deformation tongue is visible on the outer surface as the thickness reduction higher above 50% for both full annealed 2024 and 7075 aluminum alloys. However, for both solution-treated 2024 and 7075 tubes, the spin ability is lower than that of full-annealed conditions. The discrepancy between the reduction test and microscopic spin ability will be discussed in terms of the microstructure and the mechanical properties.

**Panigrahi S. et al. [19]** The effect of annealing on microstructural stability, precipitate evolution, and mechanical properties of cryorolled (CR) Al 7075 alloy was investigated in the present work employing hardness measurements, tensile test, X-ray diffraction (XRD), differential scanning calorimetry (DSC), electron backscattered diffraction (EBSD), and transmission electron microscopy (TEM). The solution-treated bulk Al 7075 alloy was subjected to cryorolling to produce fine grain structures and, subsequently, annealing treatment to investigate its thermal stability. The recrystallization of CR Al 7075 alloys started at an annealing temperature of 423 K (150 °C) and completed at an annealing temperature of 523 K (250 °C). The CR Al 7075 alloys with ultrafine-grained microstructure are thermally stable up to 623 K (350 °C). Within the range of 523 K to 623 K (250 °C to 350 °C), the size of small  $\gamma$  phase particles and AlZr<sub>3</sub> dispersoids lies within 300 nm. These small precipitate particles pin the grain boundaries due to the Zener pinning effect, which suppresses grain growth. The hardness and tensile strength of the CR Al 7075 alloys was reduced during the annealing treatment from 423 K to 523 K (150 °C to 250 °C) and subsequently it remains constant.

**Amoush A. et al. [20]** The corrosion behaviour of high strength aluminium alloy type 7075-T6 precharged with hydrogen for various charging times was investigated using electrochemical polarization and free corrosion potentials measurement techniques. The results showed that the precharged 7075-T6 aluminium alloy with hydrogen exhibited lower open-circuit (OCP) and breakdown potentials in deaerated 0.5M NaCl than those for the nonhydrogenated material. Moreover, the OCP and breakdown potentials decreased with increasing the precharging time. Microscopic observations of the exposed surfaces revealed that intergranular attack was formed in non-hydrogenated specimens whereas mixed mode of attack (i.e. intergranular and transgranular) were formed in the precharged ones during potentiostatic polarization. Moreover, the pits formed during the free corrosion potential testing were observed to be larger on the exposed surfaces of hydrogen precharged specimens. The severity of attack and pitting was observed to increase with increasing the precharging time. Consequently, the corrosion resistance of hydrogen precharged of 7075-T6 aluminium alloy with hydrogen was lower than that for non-hydrogenated material.

**LUNG B. et al. [21]** The effect of homogenization and aging treatments on the strength and the stress-corrosion cracking (SCC) resistance of the 7050 aluminum alloy has been investigated and compared with those of the same-series 7075 alloy. The recrystallized structure and the quench sensitivity are found to be significantly affected by the dispersoid distribution, depending on the homogenization conditions. The finest and densest dispersoid distribution, generated by the stephomogenization (Step-H) treatment, can effectively inhibit recrystallization to obtain the smallest fraction of recrystallized structure. Such a characteristic lowers considerably the quench sensitivity of the 7050 alloy, but it produces the reverse in the 7075 alloy. For the 7050 alloy, Step-H always exhibits the highest strength among all the aging conditions, and the proposed step-quench and aging (SQA) treatment is confirmed to achieve an optimum strength and coarsened and wide-spaced grain-boundary precipitates (GBP), which have been found to improve the resistance of the SCC by the slow-strain-rate test (SSRT). Therefore, the attainment of both optimum strength and SCC resistance is possible for the 7050 alloy via the Step-H and SQA treatment. However, such treatment is not applicable to the 7075 alloy because of its inborn high quench sensitivity.

**Nishida Y. et al. [22]** the researcher found a new-scheme ECAP process using a rotary die was applied to a SiC whisker-reinforced aluminum alloy-matrix composite. A squeeze cast 20 vol% SiC whisker/7075 alloy composite has been successfully processed by RD-ECAP. An essentially uniform distribution of SiC whiskers was achieved after 10 ECAP passes. After 10

ECAP passes at 573 K, the matrix grain size was about 1.5–2  $\mu\text{m}$ . 10 ECAP passes at 573 K were sufficient to convert the low-ductility, as-squeeze cast composite, into a superplastic composite. Elongation values up to about 175% were achieved together with the strain rate sensitivity coefficient of about 0.67.

**Dai W. et al. [23]** high-intensity ultrasonic wave was conducted into aluminum alloy 7075-T6 to observe the effect of emission waves on the weldability during inert gas tungsten arc (GTA) welding. Through the heat-affected zone (HAZ) and the weld, the ultrasonic-wave emissions with different paths are examined and directly correlated to the heating time, dwell time, cooling rate, as well as peak temperature of the thermal cycle, and to the grain growth, weld penetration, and hardness of the weldment. In addition, a methodology based on the characteristic curves of the relative amplitude ratios of the reflected longitudinal wave and vertical shear wave for improving the weldability of aluminum alloy 7075-T6 is presented.

**Hidalgo P. et al. [24]** The 7075 alloy is an Al-Zn-Mg-Cu wrought age-hardenable aluminum alloy widely used in the aeronautical industry. The alloy was accumulative roll bonded at 300  $^{\circ}\text{C}$  (573 K), 350  $^{\circ}\text{C}$  (623 K), and 400  $^{\circ}\text{C}$  (673 K), and the microstructure, texture, and hardness were investigated. Cell/(sub)grain size in the nanostructured range, typical b-fiber rolling texture, and homogeneous hardness through thickness were determined in all cases. Misorientation was different at each processing temperature. At 400  $^{\circ}\text{C}$ , the presence of elements in solid solution and the partial dissolution of the hardening precipitate lead to a poorly misoriented microstructure with a high dislocation density and a homogeneous b-fiber texture of low intensity, typical of intermediate degrees of rolling. At 350  $^{\circ}\text{C}$  and 300  $^{\circ}\text{C}$ , highly misoriented microstructures with smaller dislocation density and intense heterogeneous b-fiber rolling texture are observed, especially at 350  $^{\circ}\text{C}$ , wherein the degree of dynamic recovery (DRV) is higher. Hardness of the accumulative roll bonded samples is smaller than that of the starting material due to particle coarsening, and it is affected by solid solution and/or by fine precipitates produced by reprecipitation of the elements in solid solution.

**Horita Z. et.al. [25]** The study use equal-channel angular (ECA) pressing at room temperature, the grain sizes of six different commercial aluminum-based alloys (1100, 2024, 3004, 5083, 6061, and 7075) were reduced to within the sub micrometer range. These grains were reasonably stable up to annealing temperatures of ,2008C and the sub micrometer grains were retained in the 2024 and 7075 alloys to annealing temperatures of 300 8C. Tensile testing after ECA pressing through a single pass, equivalent to the introduction of a strain of 1 showed there

is a significant increase in the values of the 0.2 pct proof stress and the ultimate tensile stress (UTS) for each alloy with a corresponding reduction in the elongations to failure. It is demonstrated that the magnitudes of these stresses scale with the square root of the Mg content in each alloy. Similar values for the proof stresses and the UTS were attained at the same equivalent strains in samples subjected to cold rolling, but the elongations to failure were higher after ECA pressing to equivalent strains .1 because of the introduction of a very small grain size. Detailed results for the 1100 and 3004 alloys show good agreement with the standard Hall–Petch relationship.

**Neag A. et al. [26]** The microstructure and flow behaviour during thixo backward extrusion of 7075 aluminium alloy were investigated. Reheating the steel die and the aluminium billet placed into the die at the same time using an induction furnace provides rapidly a very homogeneous microstructure suitable for thixoforming. During thixoeextrusion, despite the high solid fraction, the solid globules are weakly connected and slide over each other without any plastic deformation. The flow remains quasi homogeneous resulting in homogeneous induced microstructure of the component.

**Ortiz D. et al. [27]** Aluminum alloys 6061, 2024, and 7075 were heat treated to various tempers and then subjected to a range of plastic strain (stretching) in order to determine their strain limits. Tensile properties, conductivity, hardness, and grain size measurements were evaluated. The effects of the plastic strain on these properties are discussed and strain limits are suggested.

**Pataric A. et al. [28]** The study presented an attempt to obtain the better quality of an aluminium super-high strength alloy by application of electromagnetic field during the casting process. The conventional continuous casting process of aluminum alloys causes many defects, such as surface imperfections, grain boundary segregation, non-uniform grain size, and porosity. The better ingot surface along with the homogeneous fine-grained microstructure, and hence the better mechanical properties of the ingot, can be achieved by applying the electromagnetic casting process. The microstructure characterization, accompanied by quantitative metallographic assessment, reveals that it is possible to avoid or decrease many defects of as cast ingots during electromagnetic casting process. In this article, the microstructure of the samples of as cast 7075 aluminum alloy, obtained with and without electromagnetic field influence, was analyzed by optical microscope and the variation of key alloying elements content, i.e., Zn and Mg, through the ingot cross section was examined by

chemical analysis. Besides, the microstructural parameters such as dendrite arm spacing, interdendritic space width, as well as eutecticum and intermetallic phases volume fraction, were measured using linear method. The electromagnetic field influence on the microstructure of the as cast 7075 Al alloy was evaluated based on measured quantitative metallographic data.

### **2.3 Gaps in Literature**

1. Thixoforming process has been done on different Al alloy (7XXX, 6XXX) series separately considering different range of temperature using different method for investigation of mechanical properties but no one has analyzed this process on different series of Al alloys using the same temperature range and same method.
2. Also very less research has been done in this regard on Al 6series like (Al6063, 6082).
3. So in this thesis work, the feasibility of Thixoforming process on Al alloy 6063 & 6082 will be studied and comparison of mechanical properties after performing Thixoforming process on Al alloy 6082 and Al alloy 6061 at particular temperature range using the same method will be done.
4. It is proposed to use 6- series of Al alloy for performing conventional extrusion process and Thixoforming process at particular temperatures and compare their mechanical properties.

### **2.4 Proposed Work**

It is proposed to take two aluminum alloys (i.e.6061 and 6063) and then perform direct extrusion with the help of conventional extrusion and Thixoforming process and investigate the mechanical properties and behavior of the alloys.

The Thixoextrusion process is a new method for manufacturing complicated and net shape component through which high strength materials can be formed more easily. In this study Al alloy 6082 and 6063 which has low extrude ability has been thioxform by the extrusion process. As it is known, conventional extrusion of 6082&6063 Al alloy has been very difficult due to high strength and multiphase microstructure characterization. The necessary microstructure for semisolid processing consists of non dendritic structure with the fine globular grains. There are different methods to reach desirable microstructure prior to thixoforming such as magneto hydrodynamic stirring (MHD) & thermo mechanical processing, for example strain induced melt activate (SIMA) and recrystallization and partial melting (RAP) method which are similar but distinct. In this research, by applying the advantage of

semi solid processing, the applied pressure for extrusion is decreased and the desired mechanical properties were reached near the standard predictable properties of 6082 & 6063 Al alloy under T6 tempering condition. The result of Thixoforming with one step, three step induction heating regimes are presented. In this step, the Rapid heating process for the temperature range of 540 to 580 °C is used at same die material and same ram speed. In this research, Recrystallization and Partial melting (RAP) method is applied to meet the semi solid state of material so that the applied pressure extrusion decreases and to use the single step heating process at temperature range 540 to 580°C.

**DETAILED DESCRIPTION OF EXTRUSION PROCESS****3.1 Extrusion Method**

Extrusion is defined as the process of shaping material, such as aluminum, by forcing it to flow through a shaped opening in a die. Extruded material emerges as an elongated piece with the same profile as the die opening.

**3.2 Thixoforming Process**

Thixoforming process consists of an injection into the component die of material at semisolid state. In order to get the thixotropic behavior of the material (viscosity which decreases with increase of shear stress and time), its structure before injection has to be composed of solid globular dendrites dispersed in liquid eutectic fraction (rheocast structure). Therefore the material has to be undergone at a preliminary procedure for obtaining billets having the right structure suitable for thixoforming process. More methods are available for reaching this structure: electromagnetic stirring, mechanical stirring, passive stirring, grain refinement. Electromagnetic steering is the most used for aluminium alloys. During solidification, the steering breaks the tree dendrites which solidify with spheroidal shape.

**3.2.1 Advantage of Thixoforming Process**

The advantageous attributes of Thixoforming have been described as follows:

- It is an energy efficient process which is easily automated and controlled to achieve consistency.
- Production rates are similar to pressure die casting or better.
- Smooth filling of the die with no air entrapment and low shrinkage porosity gives parts of high integrity.
- Lower processing temperatures reduce the thermal shock of the die, promote die life and allow the processing of high melting point alloys (such as tool steels and stellites) that are difficult to form by other means.
- Fine, uniform microstructures give enhanced component properties.

- Weight savings can be achieved through optimized component design.

The high mechanical, geometric and surface quality of components produced through Thixoforming can justify the removal of additional production processes such as machining steps and the need for reinforcing inserts. A simpler, more flexible production process requires fewer resources for control and allows a more rapid response to changing customer requirements. The extent to which these benefits are achieved depends upon the design of the component and its dies, the optimization of the processing conditions, the integration of the technology into an existing production process and the demands of the organization's business environment. Not only are such benefits difficult to quantify in an analysis, but they are also dependent upon managerial decisions.

### **3.2.2 Limitation of the Thixoforming Process**

A number of drawbacks currently limit the commercial viability of Thixoforming:

- The high cost of raw material and the low number of its suppliers.
- The considerable research effort and expense required to implement a viable manufacturing process due to the limited process knowledge.
- The higher die development costs than for conventional forming technologies because of the lack of available process experience and design rules.
- The higher level of training required for personnel employed to operate and maintain a Thixoforming plant compared to traditional operators.

Despite the recent development of product quality and customer service as sources of manufacturing competitiveness, in many industries cost is still regarded as the primary consideration. The relatively high price of suitable feed stock for the Thixoforming process is therefore perceived to be the major barrier to its commercialization. As these prices are related to volumes of raw material production, they are unlikely to fall until demand increases significantly.

### 3.3 Classification of Extrusion Process

There are several ways to classify metal extrusion processes. It is classified on the basis of direction, operating temperature and equipment [40].

By direction

- Direct / Indirect extrusion
- Forward / backward extrusion

By operating temperature

- Hot / cold extrusion

By equipment

- Horizontal and vertical extrusion

#### 3.3.1 Direct Extrusion

- The metal billet is placed in a container and driven through the die by the ram.
- The dummy block or pressure plate is placed at the end of the ram in contact with the billet.
- Friction is at the die and container wall requires higher pressure than indirect extrusion.

In this research work direct extrusion process follows.

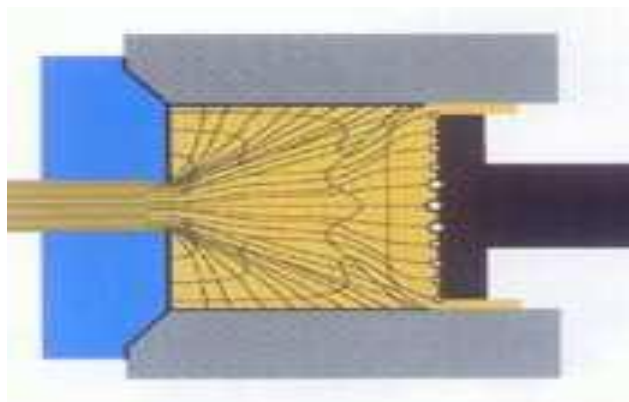


**Fig.3.1 Mechanism of Direct Extrusion [40]**

### 3.3.2 Indirect Extrusion

- The hollow ram containing the die is kept stationary and the container with the billet is caused to move.
- Friction at the die only (no relative movement at the container wall) requires roughly constant pressure.
- Hollow ram limits the applied load.

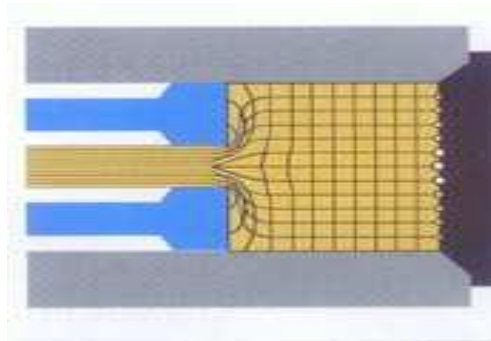


**Fig.3.2 Mechanism of Indirect Extrusion [40]**

### 3.3.3 Forward and Backward Extrusion

#### Forward Extrusion

- Metal is forced to flow in the same direction as the punch.
- The punch closely fits the die cavity to prevent backward flow of the material.

#### Backward Extrusion

- Metal is forced to flow in the direction opposite to the punch movement.
- Metal can also be forced to flow into recesses in the punch.

### 3.3.4 Cold Extrusion

Cold extrusion is the process done at room temperature or slightly elevated temperatures. This process can be used for most materials-subject to designing robust enough tooling that can withstand the stresses created by extrusion.

**Examples** of the metals that can be extruded are lead, tin, aluminium alloys, copper, titanium, molybdenum, vanadium, steel. Examples of parts that are cold extruded are collapsible tubes, aluminium cans, cylinders, gear blanks.

### **Advantage**

- No oxidation takes place.
- Good mechanical properties due to severe cold working as long as the temperatures created are below the recrystallization temperature.
- Good surface finish with the use of proper lubricants.

### **3.3.5 Impact Extrusion**

- Produce short lengths of hollow shapes, such as collapsible toothpaste tubes or spray cans.
- Requires soft materials such as aluminium, lead, copper or tin are normally used in the impact extrusion.
- A small shot of solid material is placed in the die and is impacted by a ram, which causes cold flow in the material. It may be either direct or indirect extrusion and it is usually performed on a high speed mechanical press.
- Although the process is generally performed cold, considerable heating results from the high speed deformation.

### **3.3.6 Hot Extrusion**

Hot extrusion is done at fairly high temperatures, approximately 50 to 75 % of the melting point of the metal. The pressures can range from 35-700 MPa (5076 - 101,525 psi).

- The most commonly used extrusion process is the hot direct process. The cross-sectional shape of the extrusion is defined by the shape of the die.
- Due to the high temperatures and pressures and its detrimental effect on the die life as well as other components, good lubrication is necessary. Oil and graphite work at lower temperatures, whereas at higher temperatures glass powder is used.

## **3.4 Extrusion Equipment**

Extrusion equipment mainly includes presses, dies and tooling [40].

### **Presses**

- Most extrusions are made with hydraulic presses.
- These can be classified based on the direction of travel of the ram.
  - a) Horizontal presses
  - b) Vertical presses

## **Tools**

Typical arrangement of extrusion tools.

### **Horizontal extrusion presses**

(15- 50 MN capacity or up to 140 MN)

- Used for most commercial extrusion of bars and shapes.

#### **Disadvantages:**

- Deformation is non-uniform due to different temperatures between top and bottom parts of the billet.

### **Vertical extrusion presses (3- 20 MN capacity)**

- Chiefly used in the production of thin-wall tubing.

#### **Advantages:**

- Easier alignment between the press ram and tools.
- Higher rate of production.
- Require less floor space than horizontal presses.
- Uniform deformation, due to uniform cooling of the billet in the container.

### **3.5 Advantage of Extrusion Process**

- Cross sectional shape not possible by rolling can be extruded.
- No time is lost when changing shapes since the dies may be readily removed and replaced.
- Dimensional accuracy of extruded parts is generally superior to that of rolled ones.
- The range of Extruded items is very wide: rods from 3 to 250mm in dia, pipes of 20 to 400mm in diameter and wall thickness of 1mm and above and more complicated shapes which cannot be obtained by other mechanical working method. Materials most commonly being extruded are light alloys, therefore aluminum alloys, copper, brass.
- Very large reductions are possible has compared to rolling, for which the reduction per pass (initial cross sectional area divided by the final cross sectional of the product) is generally  $\leq 2$ .
- Automation of extrusion is simpler has items are produce in a single passing.

### **3.6 Limitation of Extrusion Process**

- Process based in extrusion which consists of a poorly shaped leading and of the section and of an extruded but, is higher than rolling. It is 18 to 20% of the billet Weight in direct extrusion 5 to 6% of the billet weight in direct extrusion. Where as the wastage in rolling is only 1 to 3%.
- In homogeneity in structure and properties of an extruded product is greater due to different flow of the axial and the outer layer of blanks.
- Service life of extrusion tooling is shorter because of high contact stresses and slip rates.
- Relatively high tooling costs, being made from costly alloy steel.
- In productivity extrusion is much inferior to rolling.
- Cost of extrusion is generally greater as compared to other method.

**MATERIAL AND EQUIPMENT SPECIFICATIONS**

**4.1 Material Selection**

Extrusion process can be done on many materials such as cast iron, steel, plastics and their alloys. Aluminium and its alloys are used in a variety of cast and wrought forms and conditions of heat treatment. Forgings, sections, extrusions, sheet, plate, strip, foil and wire are some examples of wrought form, while castings are available as sand, pressure and gravity die castings.

To meet various requirements, aluminium is alloyed with copper, manganese, magnesium, zinc, nickel and silicon as major alloying elements. These alloying additions improve the properties of aluminium when added in desired percentage. The AAA (Aluminium Association of America) has classified the wrought aluminium alloys according to a four-digit system. This classification is adopted by the International Alloy Development System (IADS) and by most of the countries in the world. Table 4.1 gives the basic of designation of wrought aluminium alloys in the four digit system.

The first digit identifies the alloy type. The second digit shows the specific alloy modification. The last two digits indicate the specific aluminium alloy or the purity level in case of pure aluminium [43].

**Table 4.1 Designation of Aluminium alloys**

Alloy number	Major alloying element
1XXX	Commercially pure aluminium (99%)
2XXX	Copper
3XXX	Manganese
4XXX	Silicon
5XXX	Magnesium
6XXX	Magnesium silicide (Mg <sub>2</sub> Si)
7XXX	Zinc
8XXX	Other elements such as nickel, titanium, chromium, lead and bismuth
9XXX	Unassigned

**Table 4.2 Condition of temper of aluminium alloy can be denoted by the specific letters as**

Letter	Condition of Alloy
F	As fabricated

O	Annealed
H	Strain hardened by a cold working process
T	Heat treated

The letter H and T are generally shown with some numbers, which indicate more details about the treatment of a particular alloy. For example

**Table 4.3 Details about Strain hardened by a cold working process**

H1	Indicates only strain hardened
H2	Denotes strain hardened and partially annealed; and
H3	Signifies strain hardened and stabilized by suitable annealing

The second number 2, 4, 6, 8 or 9, if present, shows an increasing amount of strain hardening. For example, H12 denotes quarter hardened, H14 half hardened, and H18 fully hardened condition. Complete designation with treatment, for example, can be written as 5052-H18.

The different tempers produced by heat treatment are shown by letter T combined with other numbers. This tells about specific heat treatment which has been given to the alloy. The designation is as follows:

**Table 4.4 Details about Heat treated process**

T	Aged hardened
T1	Naturally aged after hot working
T2	Annealed(for casting only; for example, adopted to improve ductility of castings)
T3	Solution heat treated, cold worked and naturally aged
T4	Solution heat treated, quenched and naturally aged
T5	Artificially aged only
T6	Solution heat treated, quenched and artificial aged
T7	Solution heat treated and stabilized(by an over ageing heat treatment)
T8	Solution heat treated , cold worked and artificially aged

When talk about heat treatment for aluminium alloys, it is generally restricted to the specific operation used to improve strength and hardness precipitation hardenable wrought and cast aluminium alloys. But all aluminium alloys cannot be heat treated; such alloys are termed “non-heat treatable” alloys. Other are grouped under “heat treatable alloys”. Annealing heat treatment is carried out for both types alloys. The purpose of this treatment is to increase the

ductility. Usually, for non- heat treatable alloys, only complete or partial annealing is carried out. However, a low temperature stabilization treatment is sometimes given to 5XXX series of alloys. This treatment is designated as mill treatment. In this experiment study T6 heat treatment process used. [43]

#### 4.1.1 Heat Treatable Aluminium Alloys

Aluminum alloy of this class belong to the system with limited solubility in solid state. These are precipitation hard enable alloys. The main characteristics of this type of alloy system are temperature dependent equilibrium solid solubility, which increase with rise in temperature.

The example of this group is as follow:-

1. 2XXX series of Al-Cu alloys and Al-Cu-Mg alloys (such as 2014, 2024, 2618).Copper and magnesium improve the strength by age hardening. Nickel improves the creep resistance of the alloy.
2. 6XXX series include Al-Mg-Si type alloys. These are used as medium strength structural alloys with added advantages of good weld ability, corrosion resistance and immunity to stress corrosion cracking.6061 and 6063 T6 are common example of this series.
3. 7XXX series include Al-Zn, Al-Zn-Mg and Al-Zn-Mg-Cu type alloys. Alloys of this series show pronounced potentiality for age hardening. There is rapid decrease in solubility of zinc with decrease in temperature. Addition of copper to Al-Zn-Mg type alloy reduces the susceptibility to stress corrosion cracking. The example of this series includes 7079 and 7075 T8 which are aircraft materials.

**Table 4.5 Show the Composition, Temper, Mechanical Properties and Uses of Heat Treatable Wrought Aluminium Alloys**

Alloy Designation	Composition (%)	Temper	UTS Mpa	Yield Strength (MPa)	Elongation (%)	Shear Strength (MPa)	Fatigue Strength (MPa)	Uses
2024	4.5 Cu,1.5 Mg,0.6Mn 0.05Si,0.5Fe,0.25 Zn 0.1 Cr, 0.15Ti	O	189	77	20	126	91	Aircraft
		T36	504	400	13	294	126	structure,
		T4	476	330	20	287	140	truck
		T86	440	460	6	294		wheels
6061	1.5 Mg <sub>2</sub> Si, 0.25 Cu, 0.25 Cr	O	126	56	25	84	63	General
		T4	245	147	22	168	98	structure
		T6	315	280	12	210	98	aircraft
7075	5.6Zn,2.5Mg,1.6Cu,0.4Si, 0.5Fe,0.3Mn,0.23Cr	O	230	105	17	154		Aircraft structures

7079	0.2Ti	T6	580	510	11	336	160	As aircraft material
	4.3 Zn,3.3 Mg,0.6Cu,0.2Mn,0.2Cr	T6	545	475	14	315	160	

#### 4.1.2 Non Heat Treatable Aluminium Alloys

These alloys do not respond to heat treatment, because they consist of homogeneous solid solution with or without non coherent precipitates and show low strength and ductility. These alloys may stress hardened. Commercial, pure aluminum (1100), Al-Mn (3003), Al-Mn-Mg, Al-Si alloys are some common example of this class.

**Table 4.6 show the Composition, Temper, Mechanical properties and uses of non heat treatable aluminium Alloys**

Alloy Designation	Composition (%)	Temper	UTS (MPa)	Yield Strength (MPa)	Elongation (%)	Shear Strength (MPa)	Fatigue Strength (MPa)	Uses
1100	99% pure Aluminium	O	91	35	35	66.5	35	Packing strips, plates, cover plates, tubes
		½ H	119	98	9	77	49	
3003	1-1.5Mn,0.2 Cu,0.6Si, 0.1Zn,0.7Fe	O	92	42	30	77	49	Rigid Containers
		½ H	147	126	8	98	63	
5052	2.2-2.8Mg, 0.15-0.35Cr, 0.07Cu,0.25Si0.4Fe ,0.1Mn, 0.1Zn	O	203	98	25	126	119	Angles, gaskets, marine fittings, aircraft fuel tanks.
		½ H	259	203	10	147	133	

O= soft annealed condition

½ H= Intermediate temper obtained by varying the amount of cold work after annealing.

#### 4.2 Material Used

Based on availability and application two types of alloys are used for the present study. 6063 Aluminum alloy and 6082 Aluminium alloy are used for experimentation. The detail

description of these alloys is shown below. The all experimentation was performed in VALCO Industry Ltd. Chandigarh. The composition of these materials was checked by EDS.

#### 4.2.1 6063 Aluminum Alloy

6063 is an aluminum alloy, with magnesium and silicon as the alloying elements. The standard controlling its composition is maintained by The Aluminum Association. It has generally good mechanical properties and is heat treatable and weld able. It is similar to the British aluminum alloy HE9. Table 4.7 shows chemical composition of 6063 Aluminium alloy.

**Table 4.7 Chemical Composition of 6063 Aluminium alloy (mole %)**

Si	Fe	Cu	Mn	Mg	Cr	Ni	Zn	Ti	Pb	Al
0.458	0.166	0.0071	0.016	0.0475	0.009	0.004	0.017	0.017	0.011	98.84

6063 is mostly used in extruded shapes for architecture, particularly window frames, door frames, roofs, and sign frames. It is typically produced with very smooth surfaces fit for anodizing.

#### 4.2.2 6082 Aluminium Alloy

Aluminium alloy 6082 is a medium strength alloy with excellent corrosion resistance. It has the highest strength of the 6000 series alloys. Alloy 6082 is known as a structural alloy. In plate form, Aluminium alloy 6082 is the alloy most commonly used for machining. As a relatively new alloy, the higher strength of Aluminium alloy 6082 has seen it replace 6061 in many applications. The addition of a large amount of manganese controls the grain structure which in turn results in a stronger alloy. In the T6 and T651 temper, Aluminium alloy 6082 machines well and produce tight coils of swarf when chip breakers are used.

Aluminium alloy 6082 has very good weld ability but strength is lowered in the weld zone. When welded to itself, alloy 4043 wire is recommended. If welding Aluminium alloy 6082 to 7005, then the wire used should be alloy 5356. Table 4.8 shows chemical composition of 6082 Aluminium alloy.

**Table 4.8 Chemical Composition of 6082 Aluminium alloy (mole %)**

Si	Fe	Cu	Mn	Mg	Cr	Ni	Zn	Ti	Pb	Al
1.031	0.432	0.055	0.5	0.76	0.012	0.009	0.038	0.058	0.0097	97.1

Applications of Aluminium alloy 6082 is typically used in High stress applications Trusses, Bridges, Cranes, Transport applications, Ore skips, Beer barrels, Milk churns.

### 4.3 Equipments Used

In order to investigate the mechanical properties of aluminum alloys following instruments/ equipments are required. A detail report about these instruments/ equipments along with their application and specification has been presented in these sections.

#### 4.3.1 Melting Furnace

This furnace is used for melting raw material. These have a capacity up to 10 tons and use diesel as fuel. These machines are recognized for their durable life. The following are the features and specifications of furnace.



**Fig.4.1 Melting Furnace [Courtesy by: VALCO Steel Ltd. Chandigarh]**

- Dimension: L5300 x W3850 x H2200 mm
- Dissolve Measurement: 4cubic meters
- Dissolve Temp. : Max. 750 °C
- Burner: High pressure spraying type
- Furnace Material: Steel

### 4.3.2 Hot top - Billet Casting

It used for casting the Aluminium billet. They have a capacity ranging from 1 ton to 30 tons. The detailed specifications of these machines are:



**Fig.4.2 Hot top Billet Casting System [Courtesy by: VALCO Steel Ltd. Chandigarh]**

- Casting Mould:  $178\text{Ø} \times \text{L}6000 = 402 \text{ kg/pc}$
- Style: Hot top, lifting by wire
- Hydraulic Control: 1 HP
- Trans. motor with speed reducer: 5HP
- Casting Disc:  $178\text{Ø} \times 18 \text{ holes}$
- Aluminum Mould Seal Ring: 18 holes

### 4.3.3 Blade Heater

Blade heater is a induction furnace. Blade heater is use for Recrystallization and partial melting (RAP) process, in this furnace the material transform to partial melting state, Aluminum blade is heated temperature at  $700^{\circ}\text{C}$  for specific time in different zone.

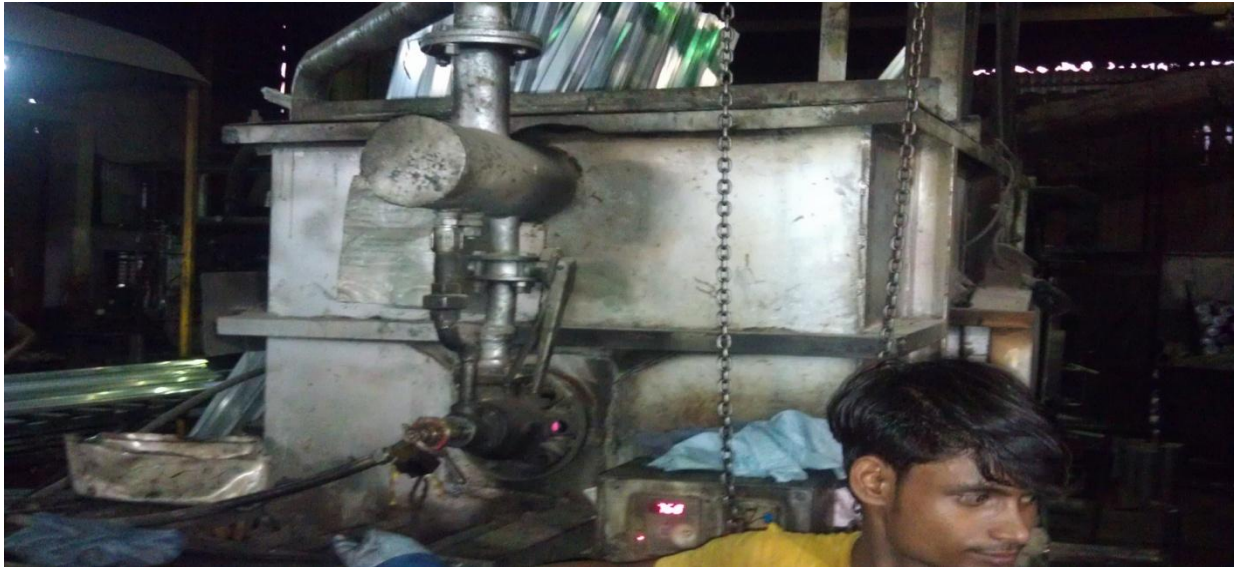


**Fig.4.3 Blade Heater [Courtesy by: VALCO Steel Ltd. Chandigarh]**

#### **4.3.4 Extrusion Press**

Most extrusions are made with hydraulic presses. These can be classified based on the direction of travel of the ram.

- a) Horizontal presses
- b) Vertical presses



**Fig.4.4 Horizontal Extrusion Press [Courtesy by: VALCO Steel Ltd. Chandigarh]**

In this experiment work, the horizontal extrusion press is used and its capacity is 880 US tonnes. In this press the maximum diameter of billet is 127mm and maximum length is 500 mm, this is one pump press and the length, width and height of pump are 900 cm, 450 cm and 350 cm respectively.

#### **4.3.5 Hydraulic Stretcher**

These machines feature a pneumatic clamp control system. Some of the technical details corresponding to extruder of these products are:

- Capacity:10 tons ~ 200 tons
- Rail: 28m(L) x 0.44m(W) x 0.6m(H)
- With Pneumatic and Hydraulic Stretcher Head and Tail Jaw System



**Fig.4.5 Hydraulic Stretcher [Courtesy by: VALCO Steel Ltd. Chandigarh]**

#### **4.3.6 Aging Heater**

Aging heater is used for T6 condition; it is heat treatment process in which material is heated at a specific temperature for specific period. The detailed specifications of these machines are:

- Design: both single and double-door are available
- Maximum Working temp: 280°C

- Production: 2-6 cases
- Heating method: electricity type
- Total electric power
- Furnace door: manually type, up and down
- Heat-preservation material: solicit acid aluminium fiber cotton
- Chamber temperature tolerance:  $\pm 5$

#### 4.3.7 Universal Testing Machine

A Universal Testing Machine, also known as a universal tester, materials testing machine or materials test frame, is used to test the tensile stress and compressive strength of materials. It is named after the fact that it can perform many standard tensile and compression tests on materials, components, and structures. The detailed specifications of these machines are:



**Fig.4.6 Universal Testing Machine [Courtesy by: CITCO. Chandigarh]**

- Capacity 100 tons
- Peak load along with on line load
- Maximum elongation with online elongation
- Ultimate Tensile Strength
- Graphical Display of elongation vs. time.
- Graphical Display of load vs. elongation
- Graphical Display of stress vs. strain.
- Complete Statistical Analysis
- Graphical Display of stress vs. strain.

#### **4.3.8 Rockwell cum Brinell hardness testing machine**

- This is a combined hardness testing machine used to measure hardness of metals & alloys of all kinds, hard or soft, whether round, flat or irregular in shapes.
- This machine is ideally suitable for laboratories, tool rooms, Heat treatment shops, R&D and Inspection Department, casting & forging industries, educational institutions.
- Rockwell & Brinell method is used for checking hardness on metals & alloys of all kinds.
- Brinell hardness is also checked on non-ferrous materials like Cast iron, Aluminum, etc.
- Automatic weight selection with automatic zero setting dial gauge.
- Rockwell test minor load is 10 kgf & major loads are 60,100,150 kgf. Brinell test for Model : MRB major load is 187.5 & for Model : MRB-250 are 187.5, 250 kgf.
- Rockwell hardness scales such as HRA, HRB, HRC, etc. Brinell hardness scale such as HB is obtained by using different types of indenters (Diamond / Ball).



**Fig.4.7 Rockwell Hardness Machine**

#### **4.3.9 Scanning Electron Microscope Machine**

Microstructure was carried out of some selected samples on Scanning Electron Microscope (SEM), model JSM-6610 LV of Jeol, Japan available at IIT, Ropar. Its resolution in high vacuum mode is 3nm. Its maximum magnification range is 3, 00,000x. SEM of samples was carried out on three ranges, namely 1000x and 1700x.

#### **4.3.10 X-Ray Diffraction Machine**

XRD analysis was carried out of some samples on X-Ray Diffraction Machine, (model ME 210 LA 2) of Rigaku corporation, Japan available at IIT, Roorkee. The range of  $2\theta$  from the  $5^\circ$  to  $100^\circ$  was used at a scan speed of  $5^\circ/\text{minute}$  for each test.

### METHODOLOGY AND PROCEDURE

#### 5.1 Procedure

The following steps briefly explain the procedure for conducting the experimentation [42].

1. Melting the raw material in melting furnace.
2. Cast the billet into hot top billet casting.
3. For RAP process (explanation provided in section 5.2) billets must be heated to approximately 700 °C.
4. After a billet reaches the desired temperature, it is transferred to the loader where a thin film of smut or lubricant is added to the billet and to the ram. The smut acts as a parting agent (lubricant) which keeps the two parts from sticking together.
5. The billet is transferred to the cradle.
6. The ram applies pressure to the dummy block which, in turn, pushes the billet until it is inside the container.
7. Under pressure the billet is crushed against the die, becoming shorter and wider until it has full contact with the container walls. While the aluminium is pushed through the die, liquid nitrogen flows around some sections of the die to cool it. This increases the life of the die and creates an inert atmosphere which keeps oxides from forming on the shape being extruded. In some cases nitrogen gas is used in place of liquid nitrogen. Nitrogen gas does not cool the die but does create an inert atmosphere.
8. As a result of the pressure added to the billet, the soft but solid metal begins to squeeze through the die opening and it is also called extrusion( explained provided in section 4.2)
9. As an extrusion exits the press, the temperature is taken with a True Temperature Technology (3T) instrument mounted on the press platen. The 3T records exit temperature of the aluminium extrusion. The main purpose of knowing the temperature is to maintain maximum press speeds. The target exit temperature for an extrusion is dependent upon the alloy. For example, the target exit temperature for the alloys 6063, 6463, 6063A, and 6101 is 930° F (minimum). The target exit temperature for the alloys 6005, and 6061 is 950° F (minimum).
10. Extrusions are pushed out of the die to the lead out table and the puller, which guides metal down the run-out table during extrusion. While being pulled, the extrusion is cooled by a series of fans along the entire length of the run-out and cooling table and

some time also cooled by water. (Note: Alloy 6061 is water quenched as well as air quenched.)

11. Not all of the billet can be used. The remainder (butt) contains oxides from the billet skin. The butt is sheared off and discarded while another billet is loaded and welded to a previously loaded billet and the extrusion process continues.
12. When the extrusion reaches a desired length, the extrusion is cut with a profile saw or a shear.
13. Metal is transferred (via belt or walking beams systems) from the run-out table to the cooling table.
14. After the aluminium has cooled and moved along the cooling table, it is then moved to the stretcher. Stretching straightens the extrusions and performs 'work hardening' (molecular realignment which gives aluminium increased hardness and improved strength).
15. The next step is sawing. After extrusions have been stretched they are transferred to a saw table and cut to specific lengths. The cutting tolerance on saws is 1/8 inch or greater, depending on saw length.
16. After the parts have been cut, they are loaded on a transportation device and moved into age ovens for aging process (explained provided in section 4.3). Heat-treating or artificial aging hardened the metal by speeding the aging process in a controlled temperature environment for a set amount of time.
17. After the aging operation ,the next important thing is studies its different mechanical properties which includes strength , hardness etc. of material(explained provided in section 4.4)

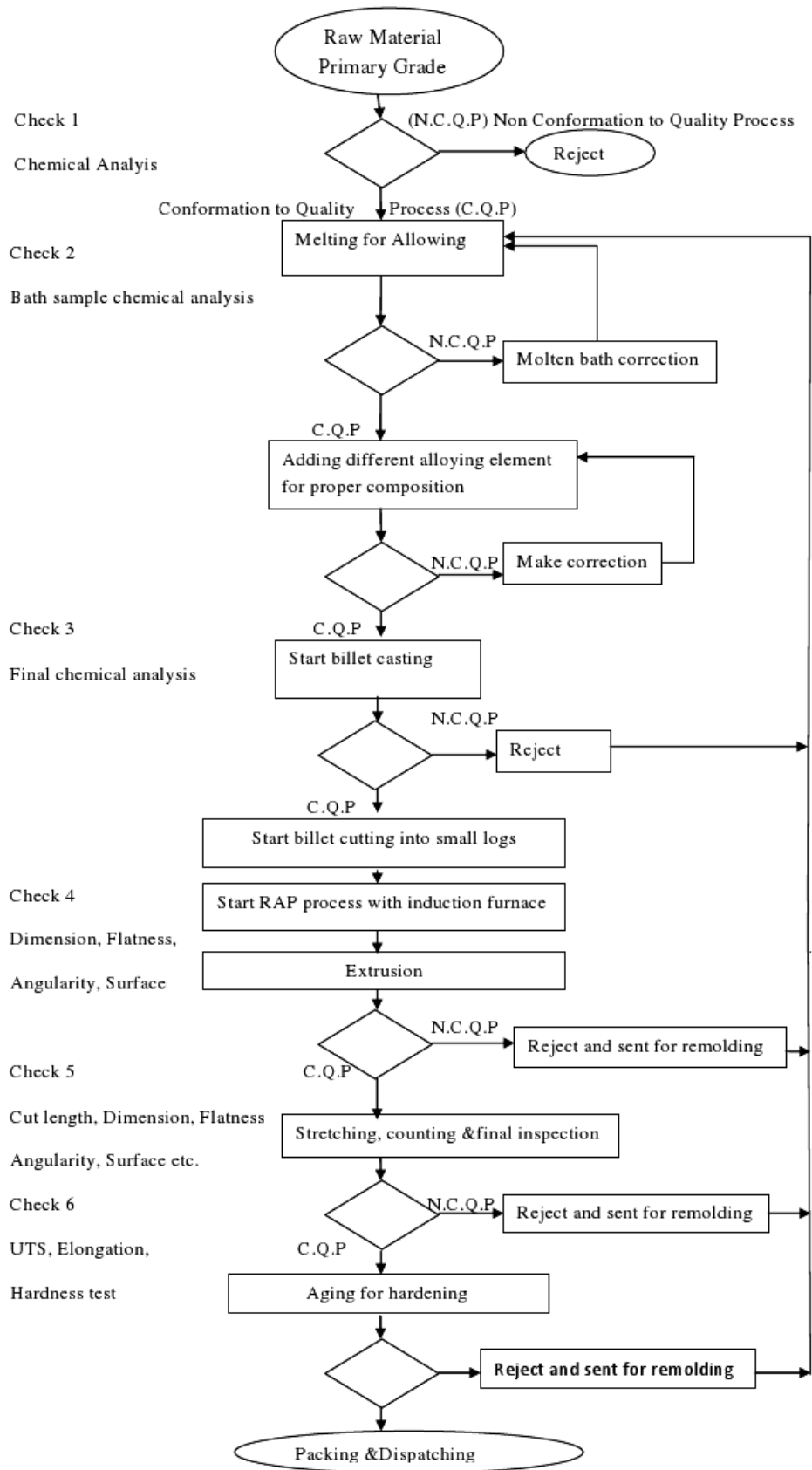


**Fig. 5.1 Flow Chart of Procedure**

### 5.1.1 Recrystallization and Partial Melting (RAP)

In RAP process raise the temperature of billet in blade heater at semi solid state, at this state metal show 30 to 40% liquid and 60 to 70% solid state. Three type of blade heaters are used in RAP process Normal heater, Induction heater and Hot log fair. In this experiment Normal heater used and reach the temperature 727°C and RAP temperature of aluminium alloys 6082 is 548°C, 585°C and 6063 is 545°C and 560 °C. The whole process explained above is summarized in the figure 5.2 [7].

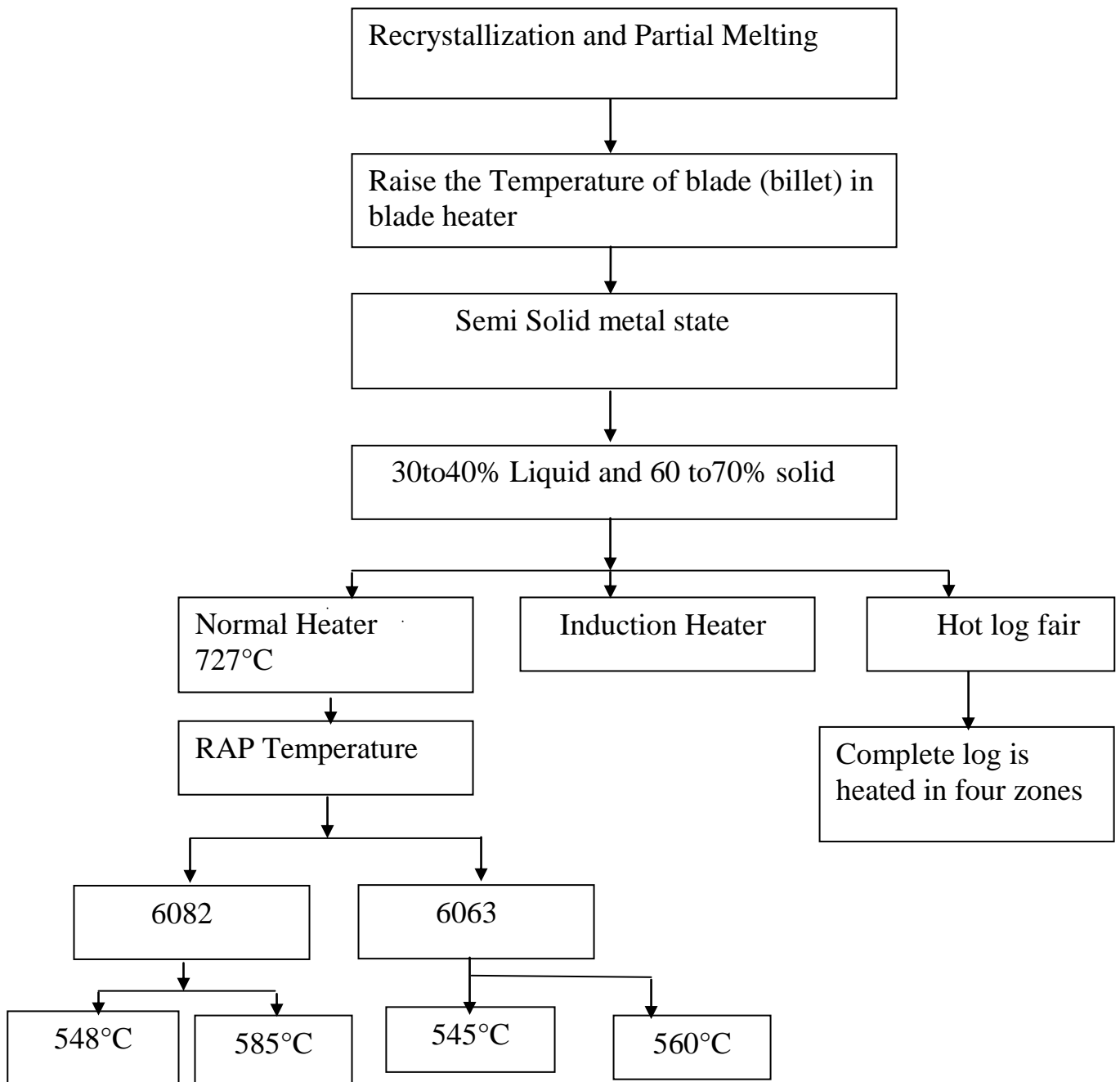


Fig.5.2 Recrystallization and Partial melting

## 5.2 Design of Extrusion Process

In extrusion process the important point is maintain the die temperature (nitrogen gas used for maintain die temperature) and container temperature equal to billet temperature to prevent the thermal shock. Then the ram applies pressure to the dummy block which, in turn, pushes the billet until it is inside the container. Then after the aluminium alloys (6082 & 6063) were extruded at different temperatures. During experimentation the ram speed and ram force were kept fixed and their value were taken as 2 to 3 mm/s and 100 to 110 kg/cm<sup>2</sup>. Figure 5.3 shows design of Extrusion process.

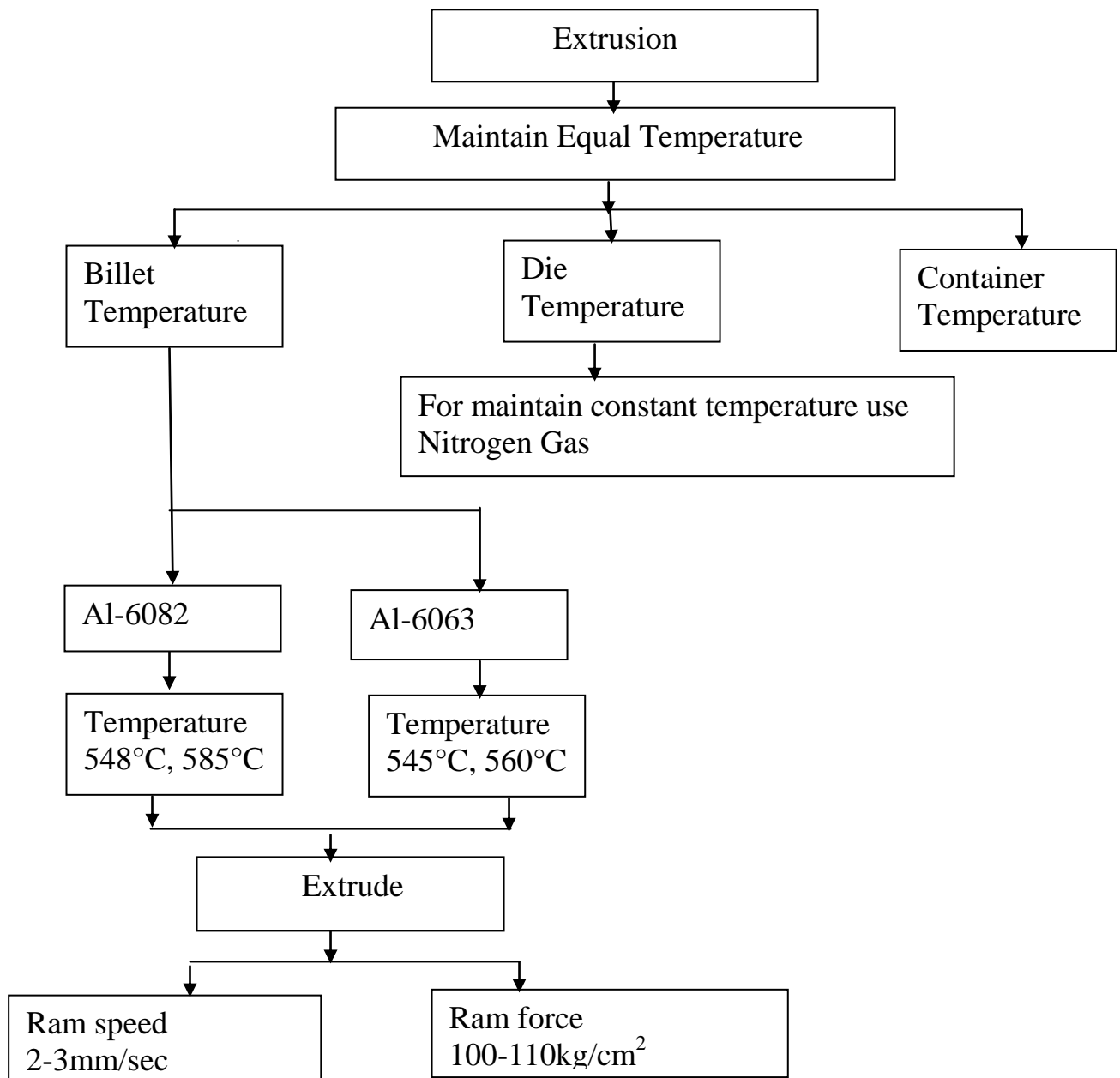
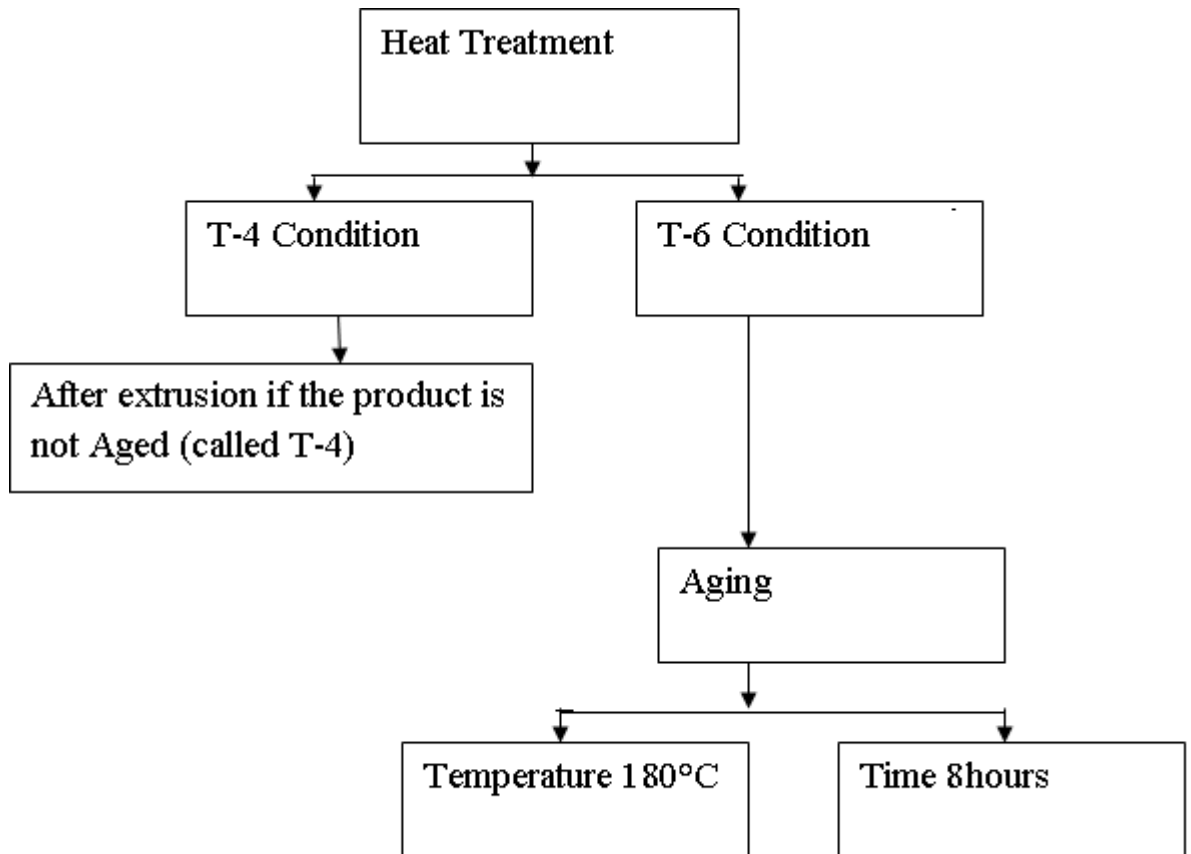


Fig.5.3 Design of Extrusion process

### 5.3 Aging Process

After extrusion, heat treatment process is done to relieve internal stresses and to enhance its mechanical properties. Heat-treating or artificial aging is a heat treatment process which hardened the metal by speeding the aging process in a controlled temperature environment for a set amount of time. In this experiment aging the metal is done at 180°C for 8 hours. The whole process explained above is summarized in the fig. 5.4.



**Fig. 5.4 Aging Process**

## 5.4 Output Parameters

The output parameters define the properties and behaviour of the material formed. Different important output parameters considered which is shown in fig 5.5

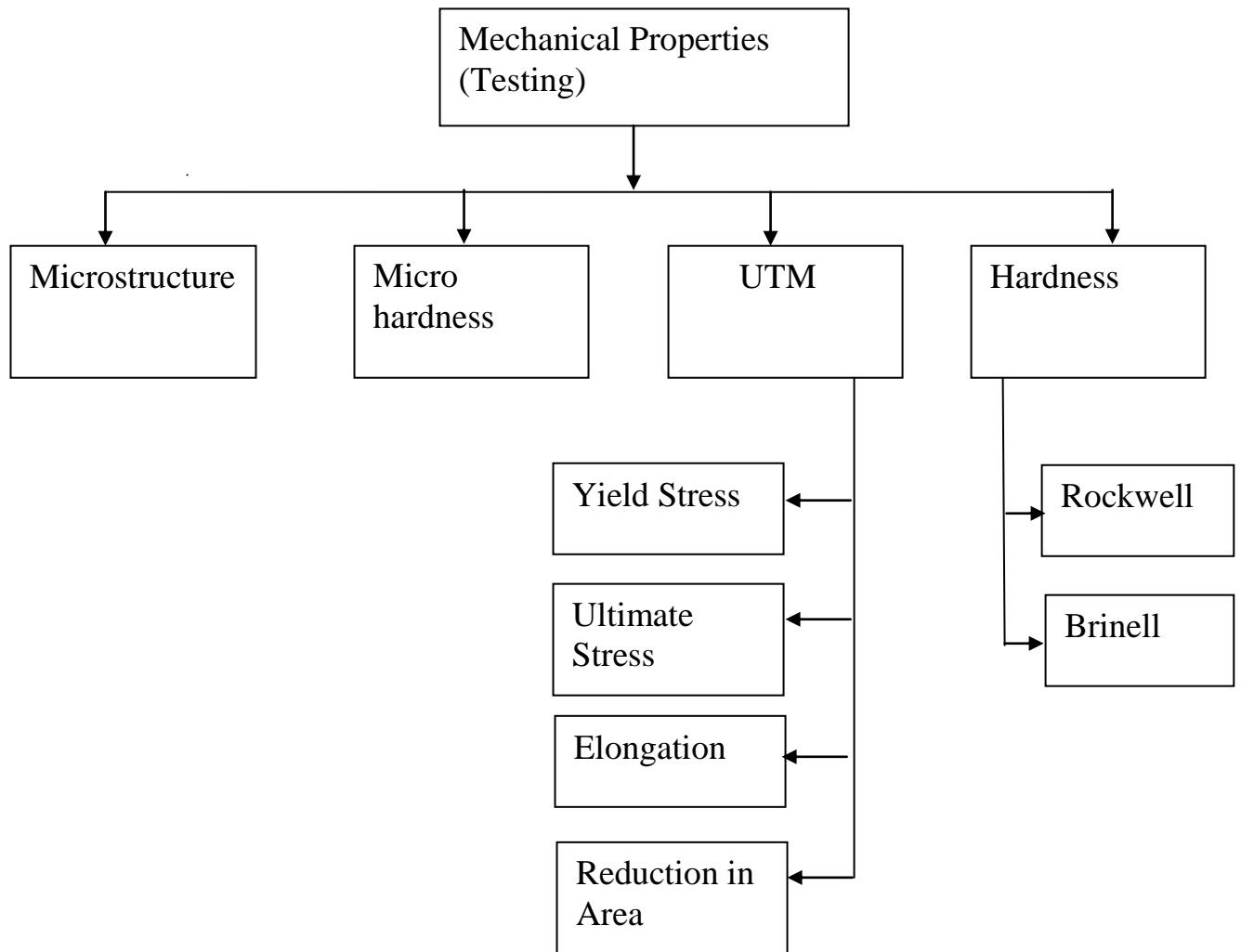


**Fig. 5.5 Output Parameters**

### 5.4.1 Tensile strength ( $R_m$ )

Stress corresponding to the maximum force [41].

### 5.4.2 Yield Strength

When the metallic material exhibits a yield phenomenon, a point during the test at which plastic deformation occurs without any increase in force [41].

### 5.4.3 Proof strength ( $R_p$ )

Stress at which total extension (elastic extension and plastic extension) is equal to a specified percentage of the extensometer gauge length [41].

**OBSERVATIONS AND ANALYSIS OF ULTIMATE TENSILE STRENGTH**

**6.1 Introduction**

In order to find the mechanical properties of the extruded material, Ultimate Tensile Stress (UTS) was done in order to find tensile strength, proof strength, upper yield and lower yield strength, elongation and percentage reduction of area. The results were found out with the help of tensile test [41].

**6.2 Analysis of UTS**

**Tensile Test**

The tensile test is used for finding UTS which is done by subjecting a test piece to a continually increase tensile strain. The tensile testing machine should be verified in accordance with IS 1828-1, and should be Class 1 or better. It should possess sufficient force capacity to break the test piece [41]. As described in the Material and Method, the process of Thixoforming, four tensile specimens by prepared from Al-6063 at temperature 545°C, similarly another four specimens were prepared from the same alloy at 560 °C.

The same procedure was followed to make four specimens of Al-6082 at 548 °C and another four specimens of same alloy at 585 °C.

**6.2.1 Preparation of test piece**

The test pieces were prepared in such a way that there is no change in its tensile properties due to heat or cold working.

The type off test piece should be as specified in the product standard. In this experiment the diameter of test pieces 10mm. For wrought products, the types of test pieces most commonly used are given in Table 6.1 below:

**Table 6.1 Show the Form, Size and Type of Test piece [41]**

Product		
Form	Size(s) <sup>1)</sup>	Type of test piece
+-		
Bars and Rods	s<4	An unmachined portion of the product
	s>4	A machined, proportional test piece

The size (s) refers to the diameter of rounds, the lateral length of squares, the width across flats of hexagons, and the thickness of flat products.

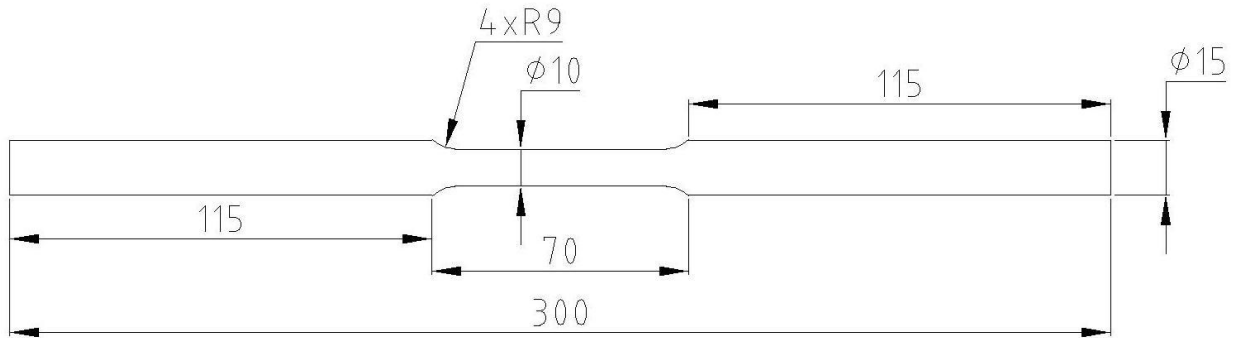


**Fig.6.1 Dimension UTM Sample**

Fig 6.1 show the different dimensions of UTM samples which is taken in this Thesis study. These dimensions are taken according to the Table 6.2.

**Table 6.2 Show the Machined, proportional test piece of circular cross section [41]**

Coefficient of proportionality k	Diameter of parallel length d (mm)	Original cross sectional area $S_0$ (mm <sup>2</sup> )	Original gauge length L = $k \sqrt{S_0}$ (mm)	Minimum parallel length $L_c$ (mm)	Minimum transition radius r (mm)	Approximately total length $L_t$ (mm)
5.65	5±0.04	19.6	25±0.25	28	6	$L_c + 2d$
	10±0.075	78.5	50±0.5	55	9	Or
	20±0.15	314	100±1	110	15	$L_c + 4d$



**Fig.6.2 UTM Samples**

## 6.2.2 Test temperature

The test should be carried out at a temperature between 10 °C and 35 °C.

## 6.2.3 Test Procedure

### 6.2.3.1 Determination of Original Cross sectional Area ( $S_o$ )

Calculate the original cross sectional area ( $S_o$ ) from the measurement of the appropriate dimensions of the test piece.

### 6.2.3.2 Marking the Original Gauge Length ( $L_o$ )

Mark each end of the original gauge length ( $L_o$ ) by means of fine marks or scribed lines, but not by notches which may cause a premature fracture. If the parallel length ( $L_c$ ) is much longer than the original gauge length, draw a series of the overlapping gauge lengths.

### 6.2.3.3 Gripping of Test Piece

Clamp the test piece in a suitable gripping device in such a way that the force is applied as axially as possible. Attach the extensometer on the test piece.

### 6.2.3.4 Loading of the Test Piece

Apply a tensile force on the test piece so as to strain the test piece in non-decreasing manner, without shock or vibration. Record the force and the corresponding extension. Accurately plot the force / extension diagram.

### 6.2.3.5 Determination of Tensile Strength ( $R_m$ )

Calculate the tensile strength ( $R_m$ ) by dividing the maximum force ( $F_m$ ) by the original cross sectional area ( $S_o$ ) of the test piece.

$$R_m = F_m / S_o \quad \text{(Equation 6.1)}$$

### 6.2.3.6 Determination of Upper Yield Strength ( $R_{eH}$ )

Calculate the upper yield strength by dividing the maximum force at the commencement of yielding by the original cross sectional area ( $S_o$ ) of the test piece.

### 6.2.3.7 Determination of lower Yield Strength ( $R_{eL}$ )

Calculate the lower yield strength by dividing the lowest value of force during plastic yielding by the original cross sectional area ( $S_o$ ) of the test piece.

### 6.2.3.8 Determination of proof strength ( $R_p$ )

Draw a line parallel to the ordinate axis (force axis) of the force / extension diagram, at a distance equal to the specified total percentage elongation, for example 0.5 %. Record the force corresponding to the point at which this line intersects the curve. Calculate the proof strength (total elongation) by dividing this force by original cross sectional area ( $S_o$ ) of the test piece.

### 6.2.3.9 Determination of percentage elongation after fracture (A)

Fit the end of a two broken pieces of the test piece together so that their axis lies in a straight line. Measure the final gauge length ( $L_u$ ) and calculate the percentage elongation after fracture from the formula given below:

$$A = \frac{L_u - L_o}{L_o} \times 100 \quad (\text{Equation 6.2})$$

### 6.2.3.10 Determination of Percentage Reduction of Area (Z)

Fit the ends of the two broken pieces of the test piece together so that their axis lies in a straight line. Determine the minimum cross sectional area after fracture ( $S_u$ ) and calculate the percentage reduction of area from the formula given below:

$$Z = \frac{S_o - S_u}{S_o} \times 100 \quad (\text{Equation 6.3})$$

## 6.3 Results for UTS

### 6.3.1 Results of tensile test of 6063 Aluminium Alloy

Table 6.3 show following mechanical properties of Aluminium 6063 alloy at temperature 545°C.

**Table 6.3 Tensile test of 6063 at temperature 545 °C**

<b>Trial No.</b>	<b>Alloy</b>	<b>Temperature (°C)</b>	<b>Ultimate Stress (N/mm<sup>2</sup>)</b>	<b>Proof Stress (N/mm<sup>2</sup>)</b>	<b>Elongation %</b>	<b>Reduction Area %</b>
1	6063	545°C	197	180.8	13.6	57.75
2	6063	545°C	230	214	14.6	57.75
3	6063	545°C	241	194	18.6	66.36
4	6063	545°C	244	226	14.8	58.23

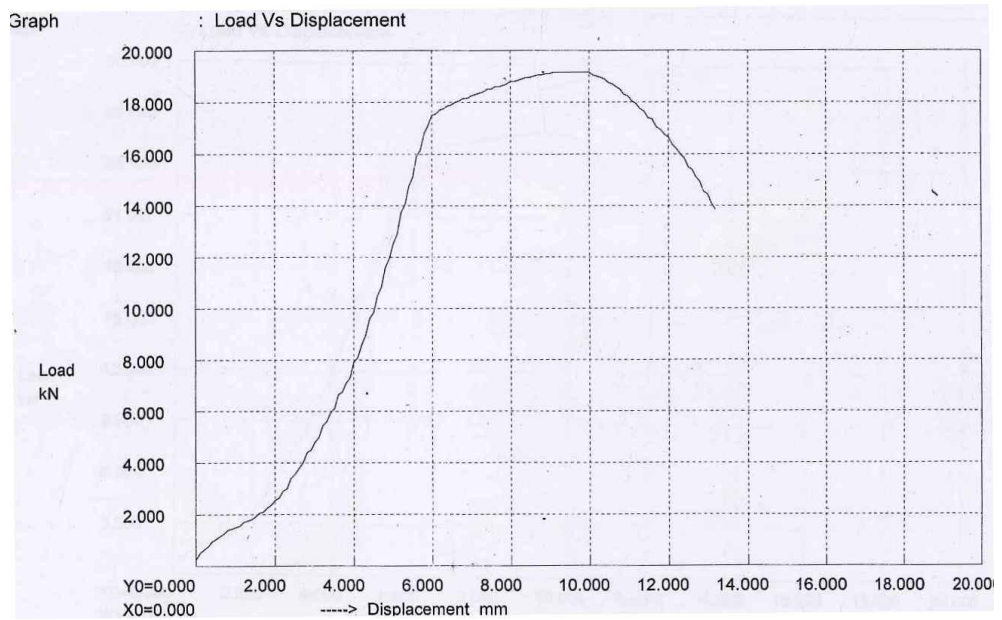


**Fig. 6.3 UTS of 6063 Al alloy at 545°C [Trail 1]**

This experiment shows that there is constant rise the displacement proportional to load till 16kN and near 18kN material show the yielding phenomena .After yielding ,material show the ultimate strength at 19kN and fracture is takes place at 14kN.

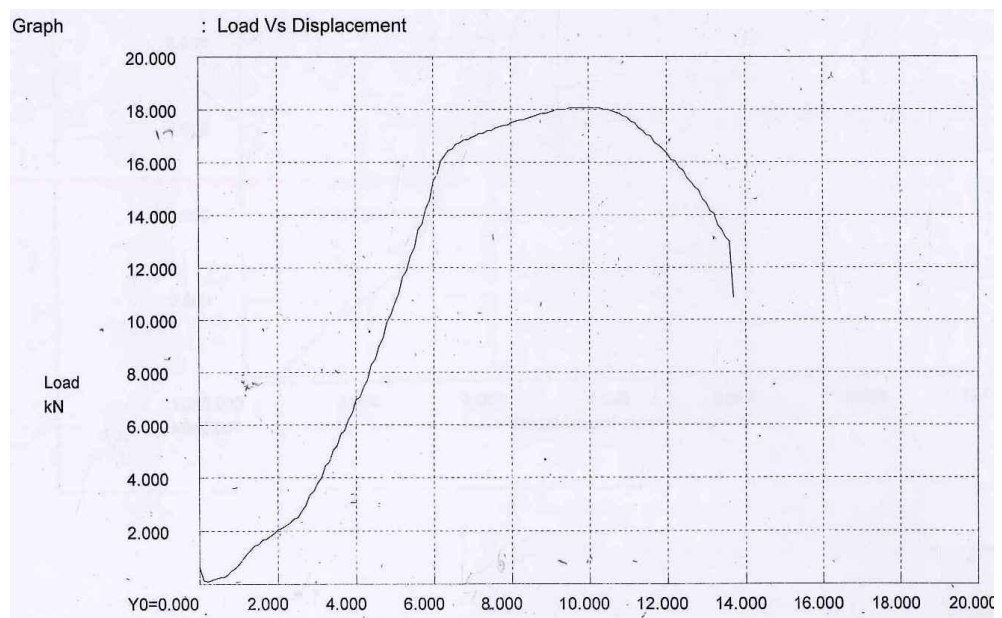


**Fig. 6.4 UTS of 6063 Al alloy at 545°C [Trail 2]**

This experiment shows that there is constant rise the displacement proportional to load till 14kN and near16kN material show the yielding phenomena .After yielding ,material show the ultimate strength at 18kN and fracture is takes place at 11kN.

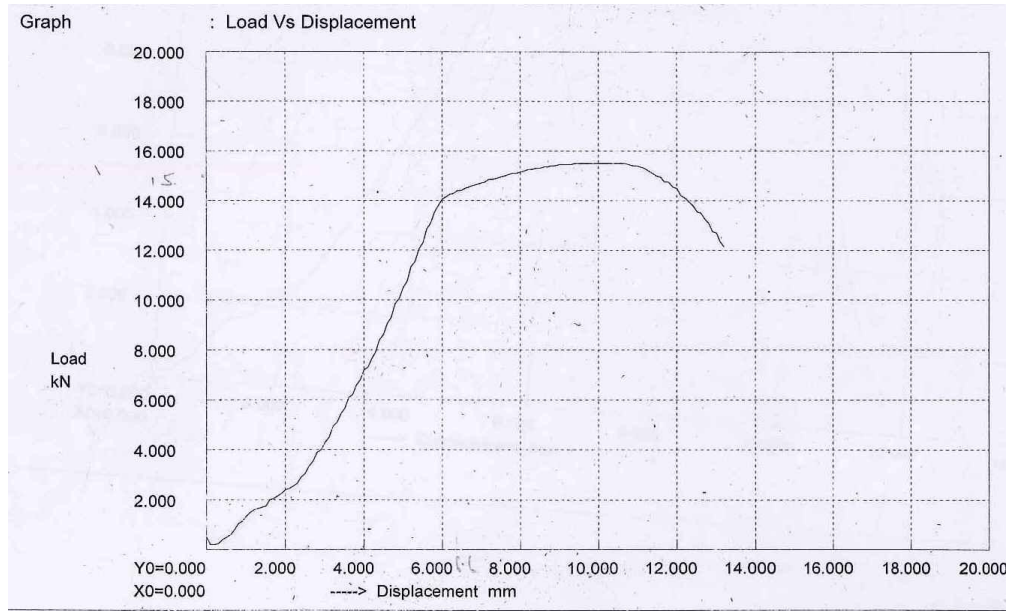


**Fig. 6.5 UTS of 6063 Al alloy at 545°C [Trail 3]**

This experiment shows that there is constant rise the displacement proportional to load till 12kN and near14kN material show the yielding phenomena .After yielding ,material show the ultimate strength at 16kN and fracture is takes place at 12kN.



**Fig. 6.6 UTS of 6063 Al alloy at 545°C [Trail 4]**

This experiment shows that there is constant rise the displacement proportional to load till 16kN and near17kN material show the yielding phenomena. After yielding, material show the ultimate strength at 19kN and fracture is takes place at 11kN.

## Tensile test of 6063 at temperature 560 °C

Table 6.4 shows following mechanical properties of Aluminium 6063 alloy at temperature 560°C.

**Table 6.4 Tensile test of 6063 at temperature 560°C**

Trial No.	Alloy	Temperature (°C)	Ultimate Stress (N/mm <sup>2</sup> )	Proof Stress (N/mm <sup>2</sup> )	Elongation %	Reduction Area %
1	6063	560°C	235	203	16	56
2	6063	560°C	251	230	14	39.16
3	6063	560°C	249	226	18	51
4	6063	560°C	260	206	12.2	49

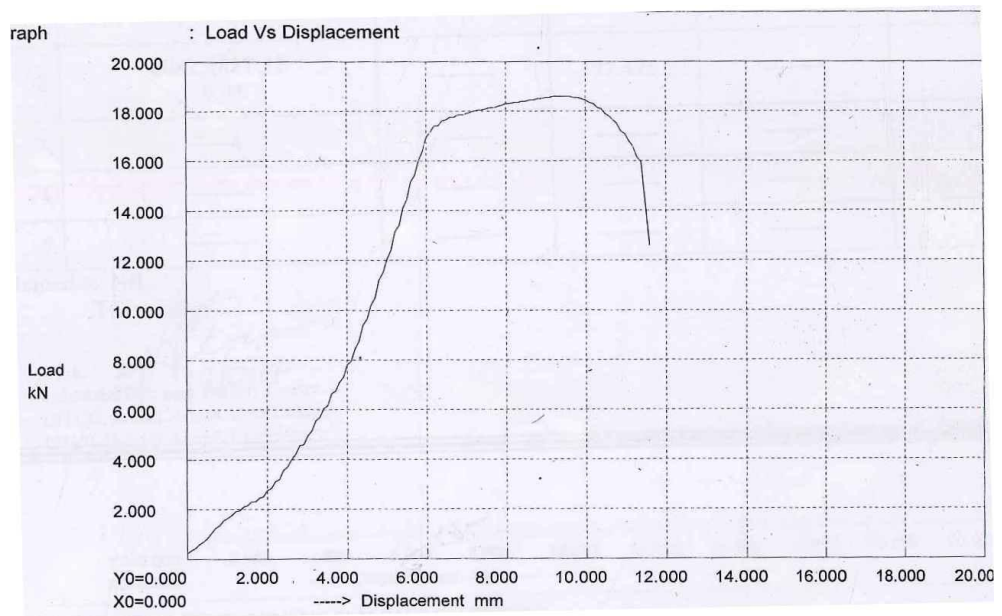


**Fig. 6.7 UTS of 6063 Al alloy at 560°C [Trail 1]**

This experiment shows that there is constant rise the displacement proportional to load till 14kN and near16kN material show the yielding phenomena .After yielding ,material show the ultimate strength at 19kN and fracture is takes place at 13kN.

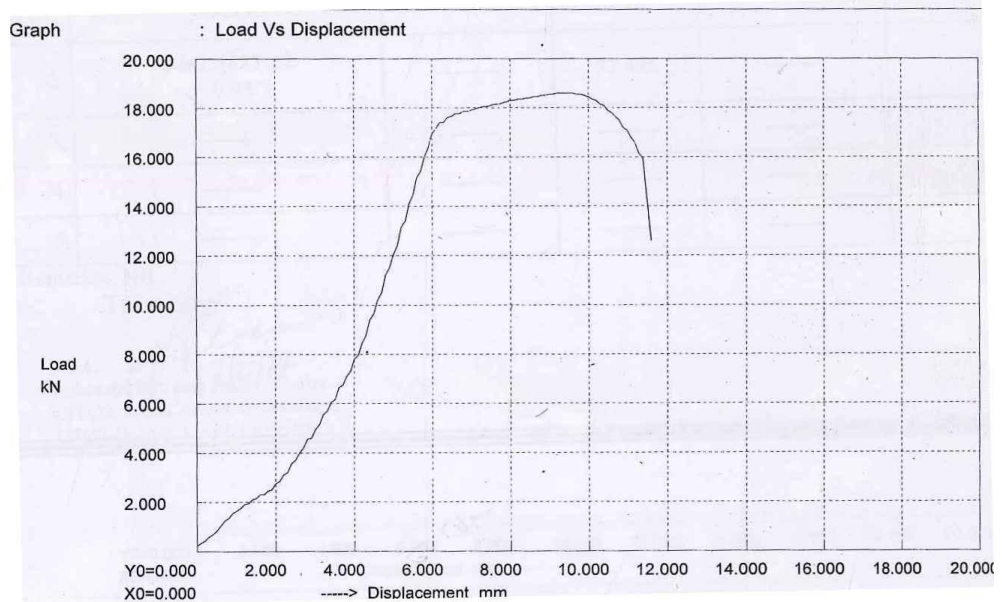


**Fig. 6.8 UTS of 6063 Al alloy at 560°C [Trail 2]**

This experiment shows that there is constant rise the displacement proportional to load till 14kN and near17kN material show the yielding phenomena .After yielding ,material show the ultimate strength at 19kN and fracture is takes place at 13kN.

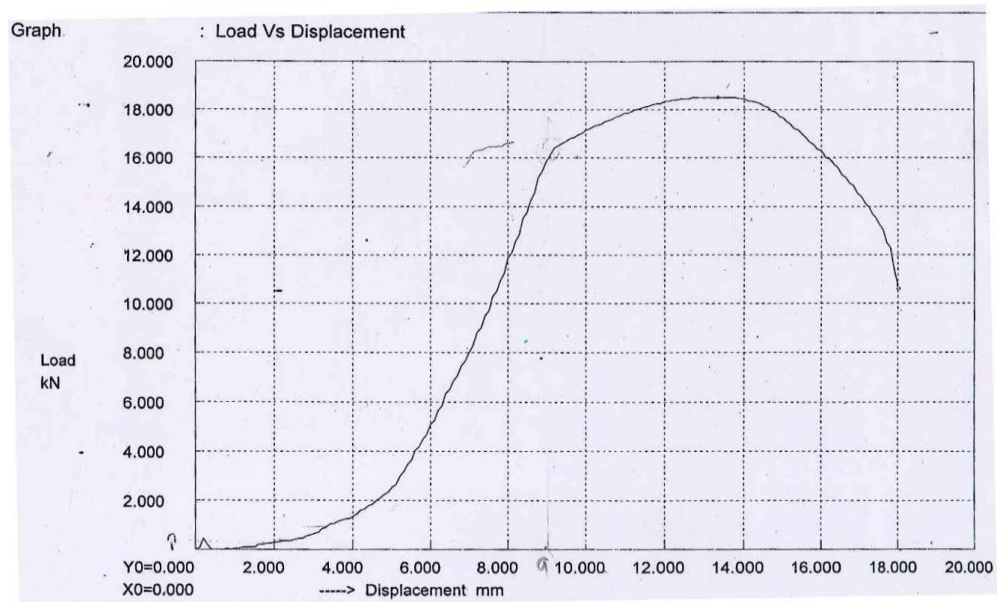


**Fig. 6.9 UTS of 6063 Al alloy at 560°C [Trail 3]**

This experiment shows that there is constant rise the displacement proportional to load till 12kN and near16kN material show the yielding phenomena .After yielding ,material show the ultimate strength at 19kN and fracture is takes place at 11kN.

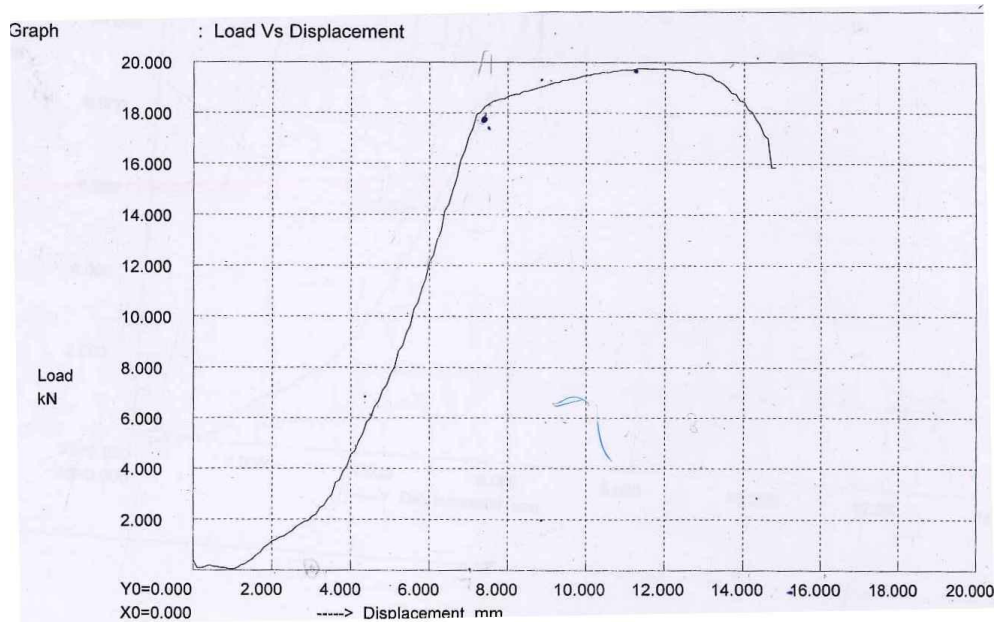


**Fig. 6.10 UTS of 6063 Al alloy at 560°C [Trail 4]**

This experiment shows that there is constant rise the displacement proportional to load till 15kN and near17kN material show the yielding phenomena .After yielding ,material show the ultimate strength at 20kN and fracture is takes place at 16kN.

### **6.3.2Results of tensile test of 6082 Aluminium Alloy**

#### **Tensile test of 6082 at temperature 548 °C**

Table 6.5 shows following mechanical properties of Aluminium 6082 alloy at temperature 548°C.

**Table 6.5 Tensile test of 6082 at temperature 548 °C**

<b>Trial No.</b>	<b>Alloy</b>	<b>Temperature (°C)</b>	<b>Ultimate Stress (N/mm<sup>2</sup>)</b>	<b>Proof Stress (N/mm<sup>2</sup>)</b>	<b>Elongation %</b>	<b>Reduction Area %</b>
1	6082	548	393	282	14.7	40.7
2	6082	548	392	233	15	48.16
3	6082	548	398	343	17	51
4	6082	548	367	303	10.5	51

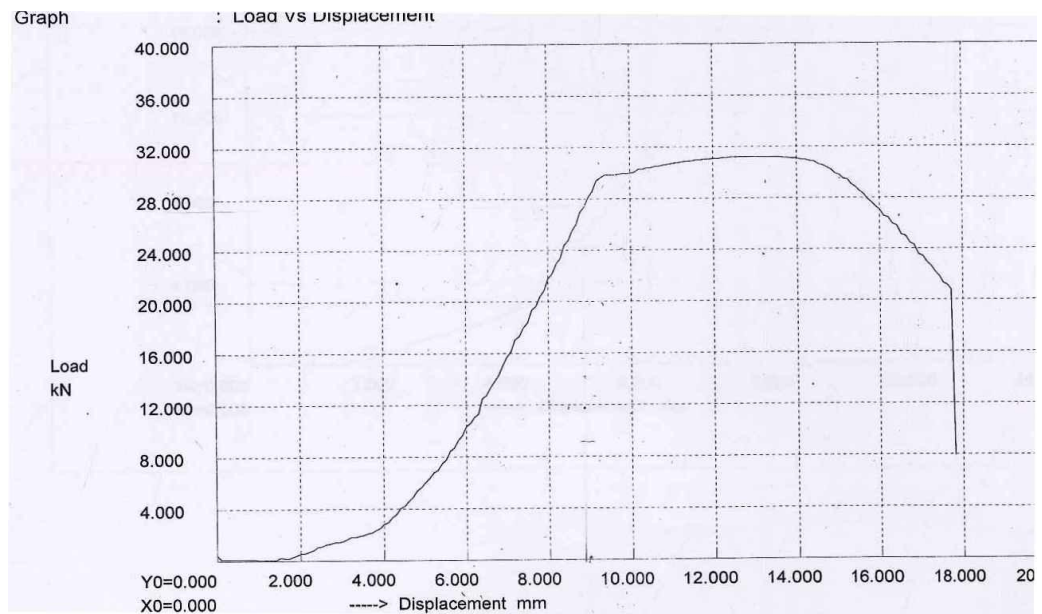


**Fig. 6.11 UTS of 6082 Al alloy at 548°C [Trail 1]**

This experiment shows that there is constant rise the displacement proportional to load till 24kN and near 26kN material show the yielding phenomena .After yielding ,material show the ultimate strength at 30kN and fracture is takes place at 9kN.

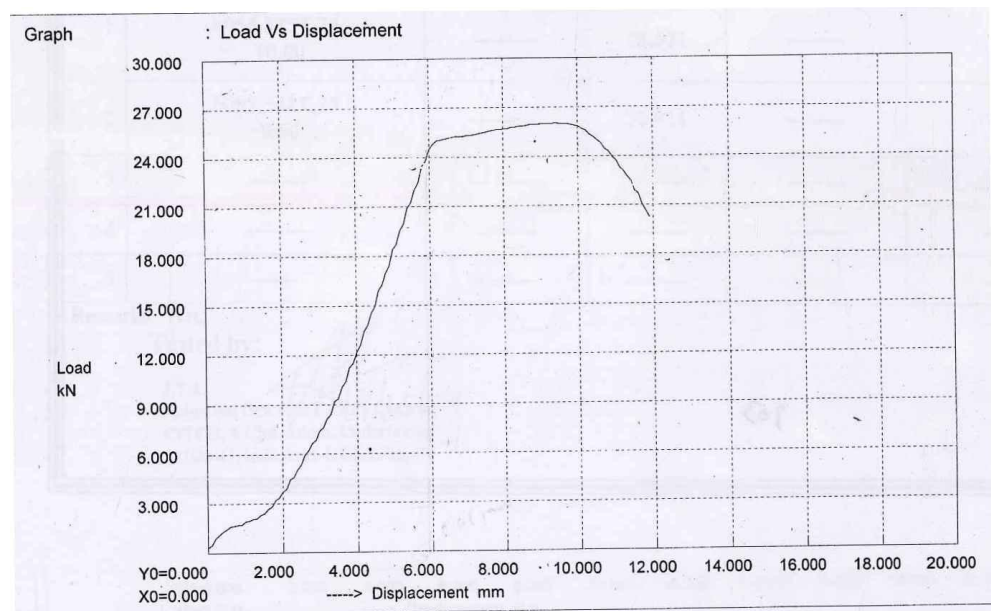


**Fig. 6.12 UTS of 6082 Al alloy at 548°C [Trail 2]**

This experiment shows that there is constant rise the displacement proportional to load till 21kN and near 23kN material show the yielding phenomena .After yielding ,material show the ultimate strength at 26kN and fracture is takes place at 19kN.



**Fig. 6.13 UTS of 6082 Al alloy at 548°C [Trail 3]**

This experiment shows that there is constant rise the displacement proportional to load till 24kN and near 27kN material show the yielding phenomena .After yielding ,material show the ultimate strength at 31kN and fracture is takes place at 11kN.

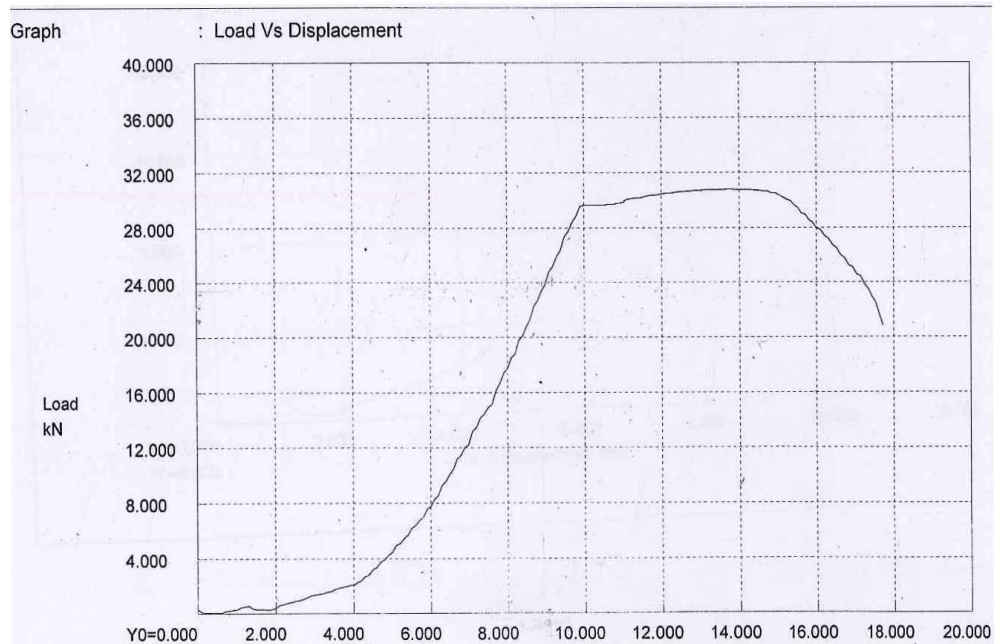


**Fig. 6.14 UTS of 6082 Al alloy at 548°C [Trail 4]**

This experiment shows that there is constant rise the displacement proportional to load till 24kN and near 26kN material show the yielding phenomena .After yielding ,material show the ultimate strength at 28kN and fracture is takes place at 19kN.

### Tensile test of 6082 at temperature 585°C

Table 6.6 show following mechanical properties of Aluminium 6082 alloy at temperature 585°C.

**Table 6.6 Tensile test of 6082 at temperature 585°C**

Trial No.	Alloy	Temperature (°C)	Ultimate Stress (N/mm <sup>2</sup> )	Proof Stress (N/mm <sup>2</sup> )	Elongation %	Reduction Area %
1	6082	585	250	231	12.2	60.62
2	6082	585	252	231	14.6	32.76
3	6082	585	239	219	15.2	37.59
4	6082	585	274	254	16	39.16

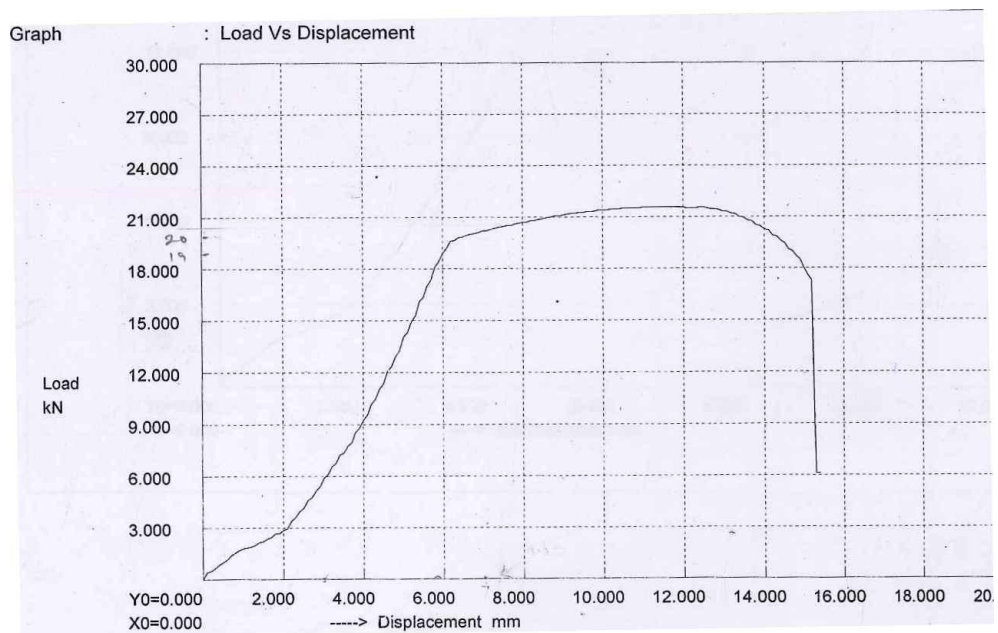


**Fig. 6.15 UTS of 6082 Al alloy at 585°C [Trail 1]**

This experiment shows that there is constant rise the displacement proportional to load till 14kN and near17kN material show the yielding phenomena .After yielding ,material show the ultimate strength at 20kN and fracture is takes place at 13kN.

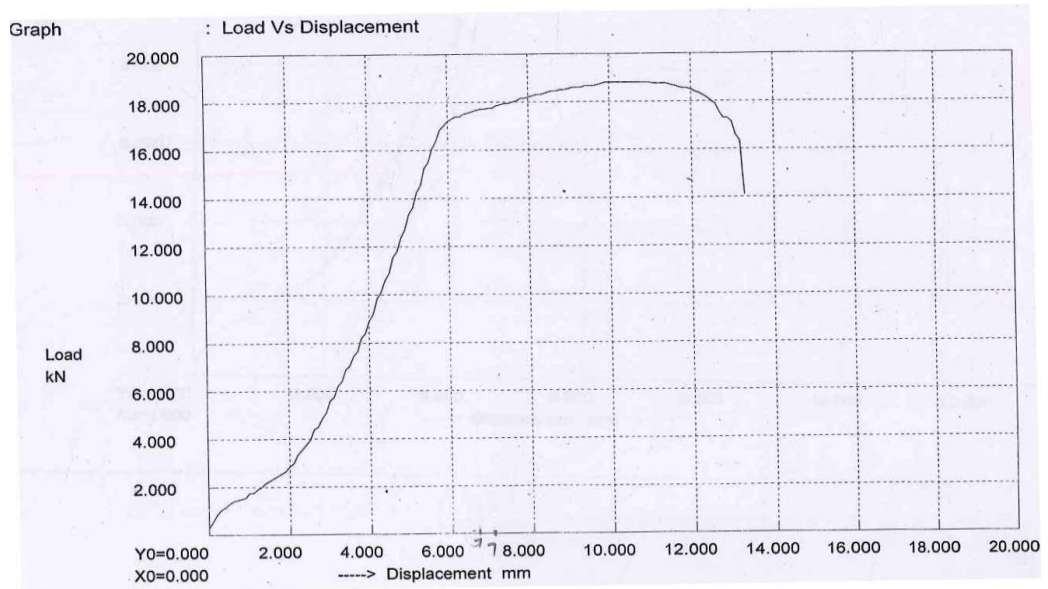


**Fig. 6.16 UTS of 6082 Al alloy at 585°C [Trail 2]**

This experiment shows that there is constant rise the displacement proportional to load till 14kN and near16kN material show the yielding phenomena .After yielding ,material show the ultimate strength at 19kN and fracture is takes place at 14kN.

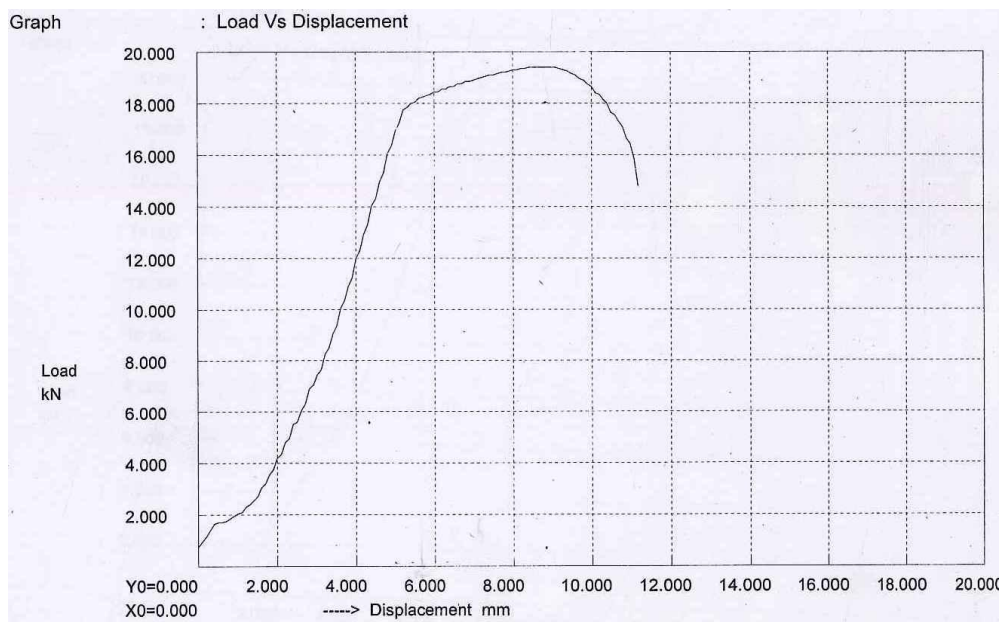


**Fig. 6.17 UTS of 6082 Al alloy at 585°C [Trail 3]**

This experiment shows that there is constant rise the displacement proportional to load till 15kN and near17kN material show the yielding phenomena .After yielding ,material show the ultimate strength at 20kN and fracture is takes place at 15kN.

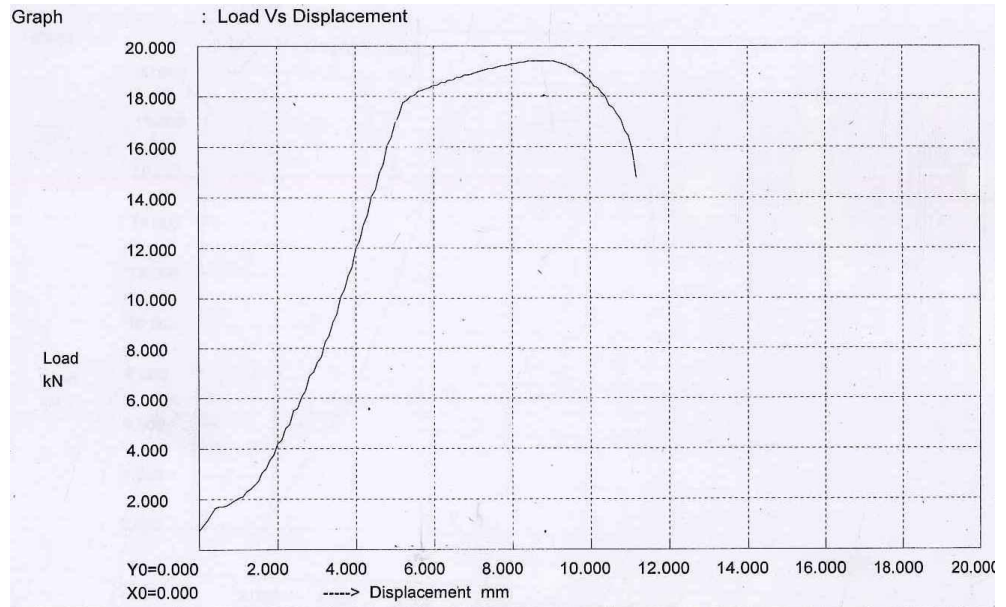


**Fig. 6.18 UTS of 6082 Al alloy at 585°C [Trail 4]**

This experiment shows that there is constant rise the displacement proportional to load till 15kN and near17kN material show the yielding phenomena .After yielding ,material show the ultimate strength at 20kN and fracture is takes place at 15kN.



**Fig.6.19 UTM Samples after break**

**OBSERVATION & ANALYSIS OF HARDNESS****7.1 Introduction**

Hardness of the work piece is found with the help of Rockwell, Brinell and Micro Hardness Tester. Rockwell and Brinell tests were performed in TERII, Kurukshetra; Micro hardness tests were carried out at Thapar University Patiala. The hardness measurement device is dependent on the diameter of indentation on the samples. The depth of penetration of an indenter under a large load is determined. The different scales, denoted by a single letter, that use different loads or indenters [41].

**7.2 Rockwell Test**

The Rockwell and Rockwell superficial hardness test are indentation hardness test in which a diamond cone having an included angle of 120° and a radius of curvature at the tip of 0.2mm or a hardened steel or hard metal ball having a diameter of 1.5875 mm or 3.175mm, is forced into the surface of a test piece in two steps, and the permanent depth of indentation under preliminary test force (minor load) after removal of the additional test force is measured.

The Rockwell hardness value is derived from the permanent depth of indentation. It is calculated by using the following formula

$$\text{Rockwell hardness value} = N - (h/S) \quad (\text{Equation 7.1})$$

Where, N= Number specific to the Rockwell hardness scale; 100 for scales A, C.

H= Permanent depth of indentation, in mm, under preliminary test force (minor load) just after removal of the additional test force, and

S= Scale unit, specific to the Rockwell hardness scales, 0.002 mm for scales A.C.

**7.2.1 Designation of Rockwell and Rockwell superficial Hardness**

For example Rockwell hardness no is 58HRC

Where, 58 = Hardness value

HR= Symbol for Rockwell hardness

C= Symbol indicating the hardness scale

**7.2.2 Apparatus****7.2.2.1 Testing Machine**

The Rockwell and Rockwell superficial hardness testing machine should comply with the requirement given in IS 1586. It should be capable of applying the test force(s). The testing

machine should be verified at planned intervals in accordance with IS 1586. For routine checking, the testing machine should be verified on each day that it is used, on a reference block with approximately the same hardness level as the material being tested.

### **7.2.3 Test conditions**

#### **7.2.3.1 Hardness Scale**

The hardness scale selected should be compatible with the type of material, the thickness of the test pieces or of the layer under test, width of area to be tested, and field of application of the hardness scale. If a choice exists between two or more hardness scales, the scale specifying the heavier total test force should be used.

### **7.2.4 Test Piece**

#### **7.2.4.1 Surface**

The top and bottom surface of the test piece should be flat, smooth and parallel. They should also be free from oxide scale and foreign matter, such as dirt and oil.

#### **7.2.4.2 Surface Preparation**

The test piece should be prepared in such a way that there is no change in the surface hardness due to heat or cold working.

#### **7.2.4.3 Thickness**

The thickness of the test piece or of the layer under test should be at least ten times the permanent depth of indentation for the diamond cone indenter, and at least 15 times the permanent depth of indentation for hardened steel or hard metal ball indenter.

### **7.2.5 Spacing of indentation**

The distance between the center of any indentation and the edge of the test piece should be at least two and a half times (2.5) the diameter of the indentation, but not less than 1mm. The distance between the centers of two adjacent indentations should be at least four times the diameter of indentation, but not less than 2mm.

### **7.2.6 Anvil**

The anvil surface in contact with the test piece should be smooth, and free from oxides scale and foreign matter, such as dirt and oil.

### 7.2.7 Test temperature

The test should be carried out at a temperature between 10 °C to 35°C.

### 7.2.8 Test Procedure

Select the appropriate Rockwell hardness scale. Place the test piece on a suitable anvil so that displacement cannot occur during the test. Bring the indenter into contact with the test surface and apply the preliminary test force in a direction perpendicular to the test surface, without shock or vibration. Set the measuring device to its datum position and, without shock or vibration, apply the additional test force. Maintain the total test force (major load) for 2 s to 6 s. While maintaining the preliminary test force (minor load), remove the additional test force and read the Rockwell hardness value directly from the measuring device after a brief period of stabilization [41].

### 7.2.9 Result and Analysis of Rockwell Hardness

Table 7.1 shows Rockwell Hardness of Al-6063 at 545°C and 560 °C with 5 repetitions.

**Table 7.1 Rockwell Hardness Result and Analysis of Al-6063**

S.No.	Alloy	Temperature	ROCKWELL HARDNESS (HRC)				
			TRAIL 1	TRAIL 2	TRAIL 3	TRAIL 4	TRAIL 5
1	6063	545°C	9	9.5	9	8	9
2	6063	545°C	10	9.5	9	9.5	8
3	6063	560°C	8.5	7.5	8	9.5	7
4	6063	560°C	9	8	8	6	10

From table 7.1 the mean value of Rockwell hardness of Al- 6063 alloy at 545°C was found

9 HRC and at 560°C was 8 HRC

Table 7.2 shows Rockwell Hardness of Al-6082 at 548°C and 585 °C with 5 repetitions.

**Table 7.2 Rockwell Hardness Result and Analysis of 6082**

S.No.	Alloy	Temperature	ROCKWELL				
			TRAIL 1	TRAIL 2	TRAIL 3	TRAIL 4	TRAIL 5
1	6082	548°C	10.5	12.5	11	13.5	12
2	6082	548°C	14.5	14	15	13.5	11
3	6082	585°C	12.5	13	12	10.5	9
4	6082	585°C	11.5	10.5	12	11	10

From Table 7.2 the mean value of Rockwell hardness of Al- 6082 alloy at 548°C was found to be 13 HRC and at 585°C was 11 HRC.

### 7.3 Brinell Hardness Test

The Brinell hardness test is an indentation hardness test in which a hard metal ball is forced into the surface of a test piece and the mean diameter of the indentation left in the surface after removal of the test force is measured.

The brinell is obtained by dividing the test force by the curve surface area of the indentation. It is calculated by using the following formula:

$$\text{Brinell hardness value} = 0.102 \times (2 \times F) / \pi \times D \times (D - \sqrt{D^2 - d^2}) \quad (\text{Equation 7.3})$$

Where, F= Test force, in N

D=Diameter of the ball, in mm

d= Mean diameter of the indentation, in mm

#### 7.3.1 Designation of Brinell hardness

For example if the designation is represented by:-

500 HBW 1/30/ 20

It means 500=hardness value

HBW= Symbol for Brinell hardness

1= Diameter of the ball, in mm

30=Solidus (/) follow by a number representing 0.10 times the test force, in N.

20= Solidus follow by the duration of application of test force, in s, in different from 10s to 15s.

### **7.3.2 Apparatus used**

#### **7.3.2.1 Testing Machine**

The Brinell hardness testing machine should comply with the requirement given in IS 2281. It should be capable of applying the test force(s). The testing machine should be verified at planned intervals in accordance with IS 2281. For routine checking, the testing machine should be verified on each day that it is used, on a reference block with approximately the same hardness level as the material being tested.

### **7.3.3 Test Condition**

#### **7.3.3.1 Force- Diameter ratio**

Force diameter ratio should be compatible with the type of material and the hardness of the test piece. It is calculated by using the following formula:

$$\text{Force diameter ratio} = 0.102 \times F/D^2 \quad (\text{Equation 7.5})$$

Where, F= Test force, in N.

D= Diameter of the ball, in mm.

#### **7.3.3 2 Test Force**

The test force should be chosen to insure that the diameter of the indentation lies in the range 0.25 to 0.60 times the ball diameter. If a choice exists between two or more test forces , the heavier test force should be used.

#### **7.3.3.3 Indenter**

Hard metal ball of diameter 1mm, 2.5 mm, 5mm or 10mm should be used. The diameter of the hard metal ball should be as large as possible in order to test the largest represented area of the test piece.

### **7.3.4 Test Piece**

#### **7.3.4.1 Surface**

The top and bottom surface of the test piece should be flat, smooth and parallel. They should also be free from oxide scale and foreign matter, such as dirt and oil.

#### **7.3.4.2 Surface Preparation**

The test piece should be prepared in such a way that there is no change in the surface hardness due to heat or cold working.

#### **7.3.4.3 Thickness**

The thickness of the test piece should be at least eight times the depth of indentation for the diamond cone indenter, and at least 15 times the permanent depth of indentation for hardened steel or hard metal ball indenter.

The depth of indentation is calculated by using the following formula

$$h = D - \sqrt{D^2 - d^2} / 2 \quad \text{(Equation 7.6)}$$

$$= 0.102 \times F / \pi \times D \times \text{HBW} \quad \text{(Equation 7.7)}$$

Where, h= Depth of indentation, in mm

D= Diameter of the ball, in mm

d= Mean diameter of the indentation, in mm

F= Test force, in N

HBW= Brinell hardness value

#### **7.3.5 Spacing of Indentation**

The distance between the center of any indentation and the edge of the test piece should be at least two and a half times (2.5) the mean diameter of the indentation. The distance between the centers of two adjacent indentations should be at least three times the mean diameter of indentation.

#### **7.3.6 Anvil**

The anvil surface in contact with the test piece should be smooth, and free from oxides scale and foreign matter, such as dirt and oil.

#### **7.3.7 Test temperature**

The test should be carried out at a temperature between 10 °C to 35°C.

#### **7.3.8 Test Procedures**

Select the appropriate test force and ball diameter.

Place the test piece on a suitable anvil so that displacement cannot occur during the test. Bring the indenter into contact with the test surface and apply the test force in a direction perpendicular to the surface, without shock or vibration. Maintain the test force for 10 s to 15 s,

unless otherwise specified. Remove the test force. Measure the diameter of the indentation in two directions at right angle to each other and calculate the arithmetic mean of the two reading. Calculate the Brinell hardness value from the formula given section 1 or read directly from the calculation tables given in IS 10588 [41].

### 7.3.9 Results and Analysis of Brinell Hardness

Table 7.3 shows Brinell Hardness of Al-6063 at 545°C and 560 °C with 5 repetitions.

**Table 7.3 Brinell Hardness Result and Analysis of Al-6063**

S.No.	Alloy	Temperature	BRINELL HARDNESS(HBW)				
			TRAIL 1	TRAIL 2	TRAIL 3	TRAIL 4	TRAIL 5
1	6063	545°C	83.9	83.9	92.8	90.7	95
12	6063	545°C	93	90.7	84	89	91.5
3	6063	560°C	84.9	76.3	77.1	81.3	84.9
4	6063	560°C	79.7	82	83.6	83	81.3

From Table 7.3 the mean value of Brinell hardness of Al- 6063 alloy at 545°C was found to be 88 HBW and at 560°C was 82 HBW.

Table 7.4 shows Brinell Hardness of Al-6082 at 548°C and 585 °C with 5 repetitions.

**Table 7.4 Brinell Hardness Results and Analysis of 6082**

S.No.	Alloy	Temperature	BRINELL(HBW)				
			TRAIL 1	TRAIL 2	TRAIL 3	TRAIL 4	TRAIL 5
1	6082	548°C	106	112	118	107	107
2	6082	548°C	109	113	106	118	108
3	6082	585°C	87	88.7	86.8	86.8	87
4	6082	585°C	89	87	86.8	83.4	85

From Table 7.4 the mean value of Brinell hardness of Al- 6082 alloy at 548°C was found to be 110 HBW and at 585°C was 87 HBW.

## 7.4 Micro Hardness Tester

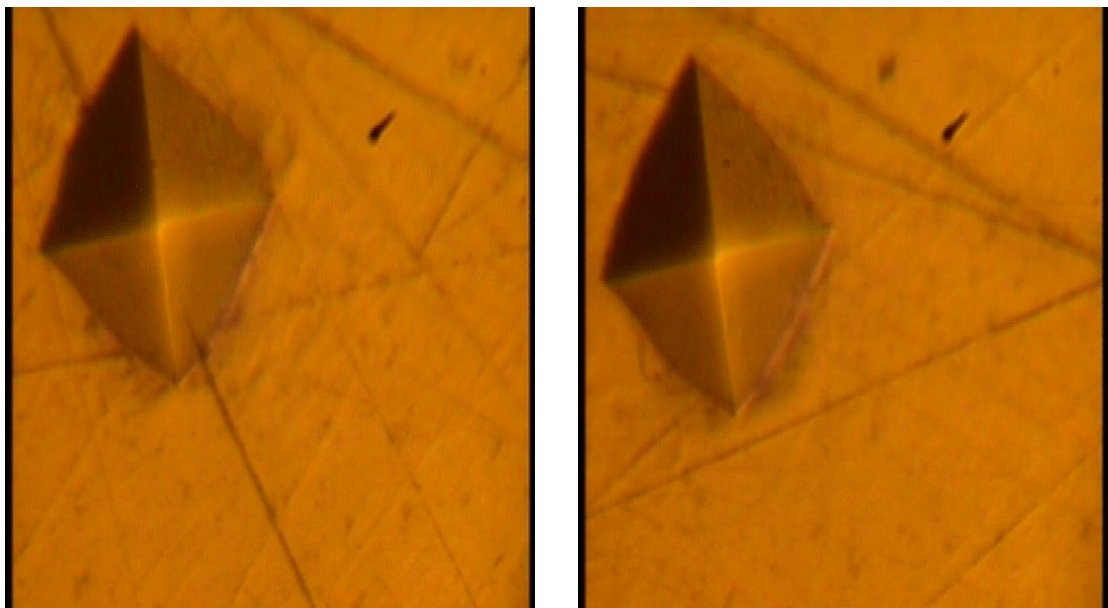
Micro hardness was measured on a computer interfaced Micro Hardness Tester,( model MVH-2) Metatech Industries, Pune , India. The micro hardness measurement is dependent on the diameter of indentation on the samples. The indent formed in the pyramid shaped indenter was measured with Quantimet software using a load of 300gm for 20 seconds. The sample is the circular shape and dimension of the sample is 15mm×5mm.

Table 7.5 shows Micro Hardness of Al-6063 at 545°C and 560 °C with 5 repetitions.

**Table 7.5 Micro Hardness Result and Analysis of Al-6063**

S.No.	Alloy	Temperature	Micro Hardness(VH)				
			TRAIL 1	TRAIL 2	TRAIL 3	TRAIL 4	TRAIL 5
1	6063	545°C	21.6945	19.5956	23.32047	21.8753	20.6474
2	6063	545°C	21.4758	23.4784	20.7446	18.7474	22.7843
3	6063	560°C	21.7682	20.2488	22.72499	21.43637	21.4847
4	6063	560°C	20.45732	21.08463	20.7563	21.73756	20.66473

From table 7.5 the mean value of Micro hardness of Al- 6063 alloy at 545°C was found to be 21.536 VH and at 560°C was 21.580687 VH.



**Fig.7.1 (a) Indentation on Al-6063 at 545°C Fig.7.1 (b) Indentation on Al-6063 at 560 °C**

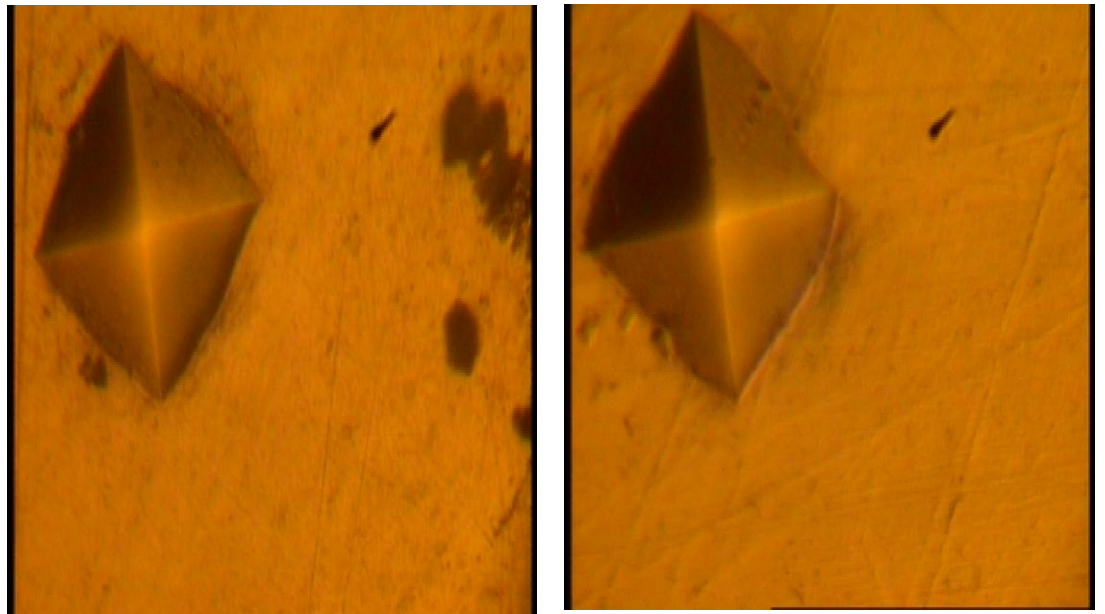
The above figures show the diamond indentation marks on Al-6063 alloy at temperature 545°C and 560 °C respectively.

Table 7.6 shows Micro Hardness of Al-6082 at 548°C and 585 °C with 5 repetitions.

**Table 7.6 Micro Hardness Result and Analysis of Al-6082**

S.No.	Alloy	Temperature	Micro Hardness				
			TRAIL 1	TRAIL 2	TRAIL 3	TRAIL 4	TRAIL 5
1	6082	548°C	26.81097	25.29965	26.74777	25.82304	26.6709
2	6082	548°C	24.7874	25.8963	26.0947	26.35857	24.8764
3	6082	585°C	23.57356	21.27037	21.36136	22.6738	23.5374
4	6082	585°C	22.5478	21.47848	22.84744	23.3729	21.74846

From Table 7.6 the mean value of Micro hardness of Al- 6082 alloy at 548°C was found to be 26.28613 VH and at 585°C was 22.06843VH.



**Fig.7.2 (a) Indentation on Al-6082 at 548 °C Fig.7.2 (b) Indentation on Al-6082 at 585°C**

The above figures show the diamond indentation marks on Al-6082 alloy at temperature 548°C and 585°C respectively.

**SEM AND XRD ANALYSIS****8.1 Introduction**

Further analysis of the machined surfaces after confirmation experiments was performed to find out surface morphology and microstructure and it has been presented in this part. Surface composition was determined with the help of X-Ray Diffraction (XRD) analysis and micro structural studies were carried out on a Scanning Electron Microscope (SEM). In this work, the effect of input parameter i.e. temperature on the surface properties of the thixoformed material were evaluated. The chemical composition of the thixoformed surface was determined with the help of X-Ray Diffraction (XRD) analysis. Micro structural analysis was carried using Scanning Electron Microscope (SEM). During this analysis, chemical composition of thixoformed surface and microstructure of thixoformed surface was evaluated.

**8.2 Microstructure Analysis**

Microstructure analysis was carried out on four selected samples using Scanning Electron Microscope to study the change in microstructure after experimentation. The samples were prepared as per standard before SEM analysis on three different magnifications namely 1000 x and 1700x.

**8.2.1 Preparing Samples for SEM**

The steps for the preparation of sample for SEM are given below:

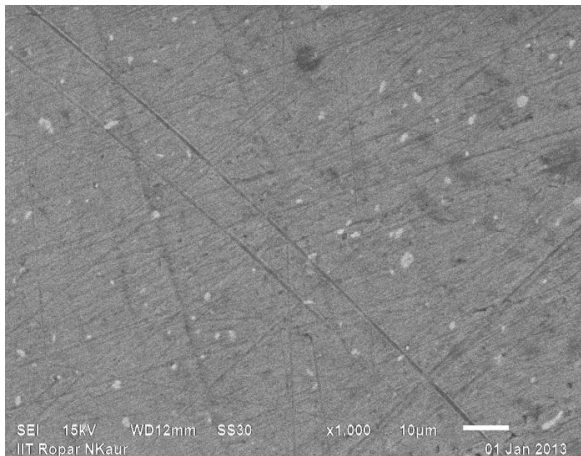
All the samples are cut into size of  $\phi$  15 mm.

Clean the surface of sample with wire brush

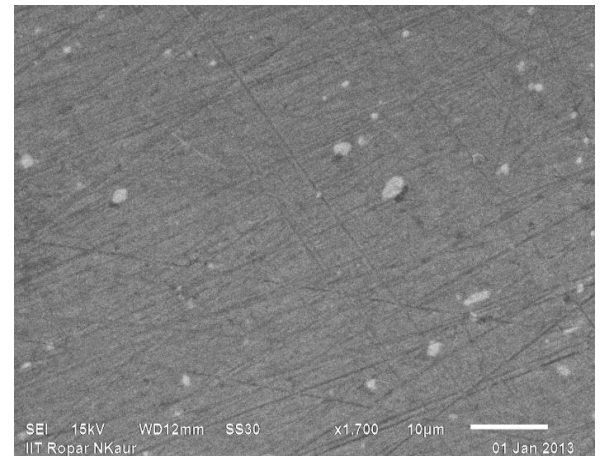
Clean the samples with acetone using cotton so as to remove debris from the machined surface.



Fig 8.1 SEM Samples

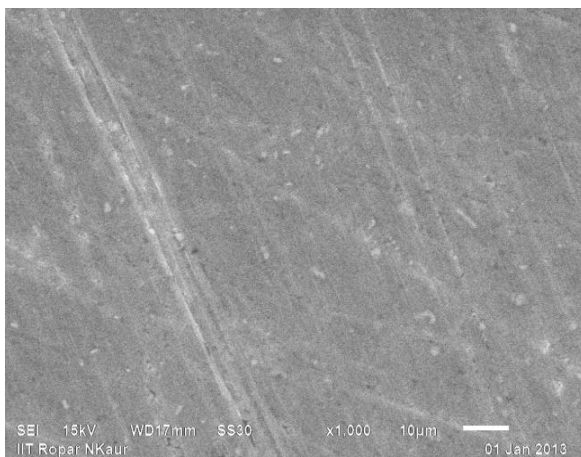


(a) At 1000 x

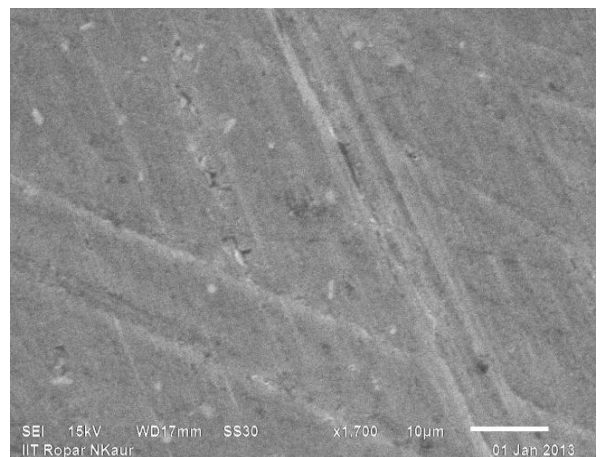


(b) At 1700 x

**Fig 8.2 SEM Analysis of Al-6082 at temperature 548°C**

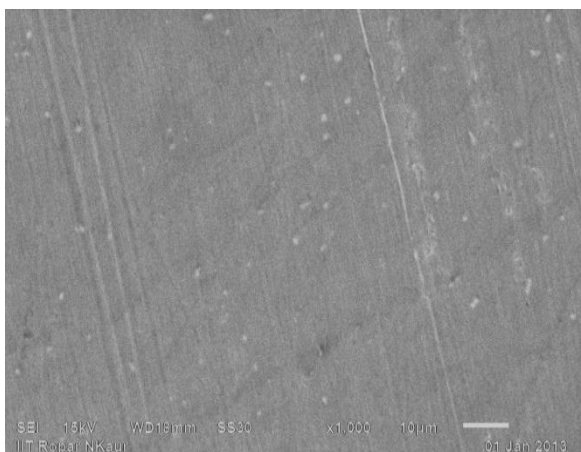


(a)At 1000x

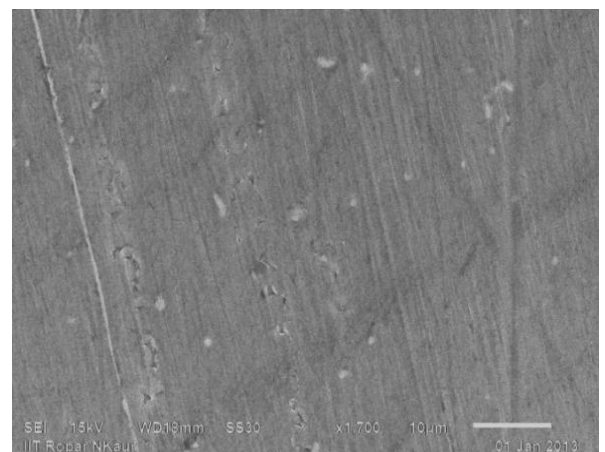


(b) At 1700x

**Fig 8.3 SEM Analysis of Al-6082 at temperature 585°C**

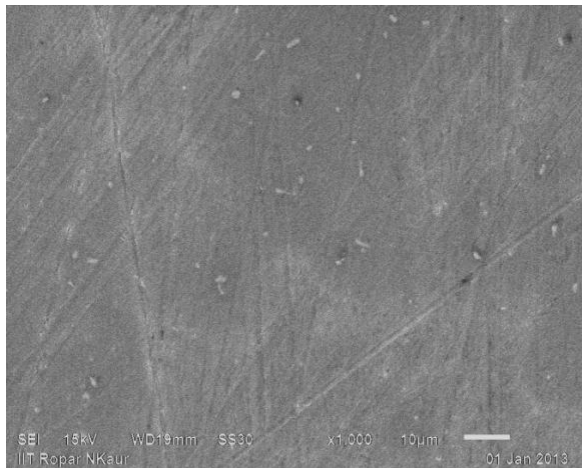


(c) At 1000X

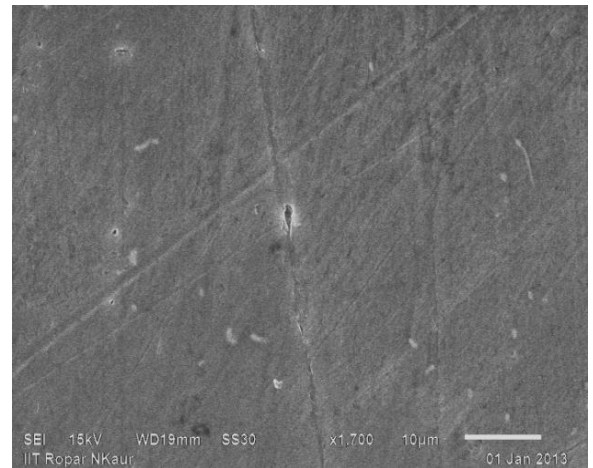


(d) At 1700X

**Fig 8.4 SEM Analysis of Al-6063 at temperature 545°C**



(a) At 1000x



(b) At 1700x

### Fig 8.5 SEM Analysis of Al-6063 at temperature 560°C

The general microstructural characteristics of the billets in the as cast condition are displayed in the above figures. The microstructure of wrought 6 series Aluminium alloy consists of elongated grains with stringers of intermediate particle. Recrystallization had occurred with liquid penetration of the boundary. But there are some unrecrystallised grains. Single step heating gives fully recrystallised structure if hold at 550-580° C. The apparent quantity of liquid is less than that present at temperature because the quench rate is insufficient to prevent some solidification on to the spheroids during cooling.

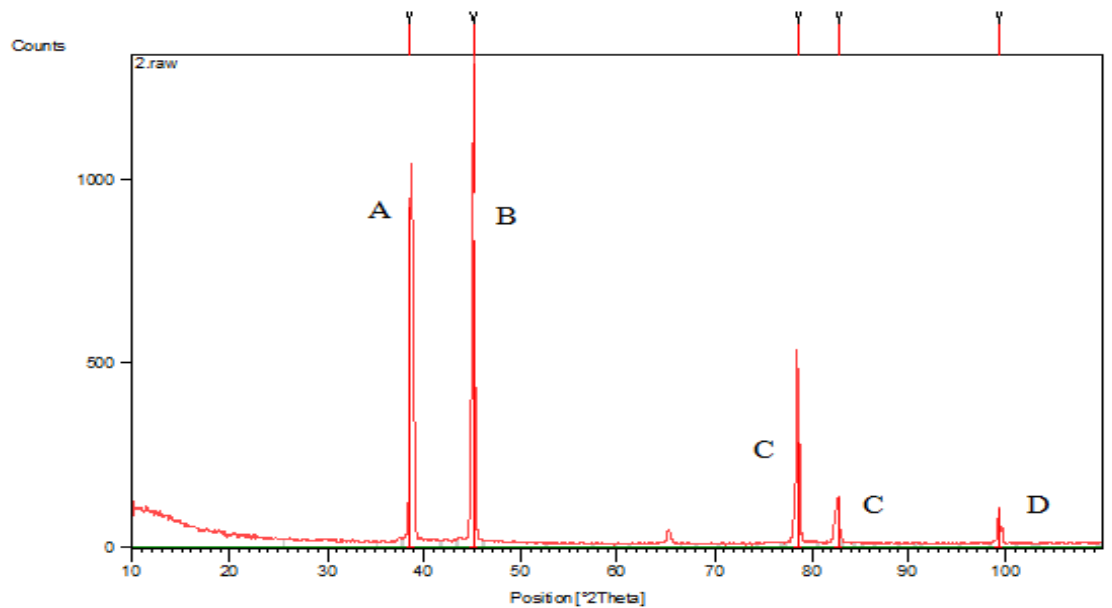
It is clearly observed from above figures that solute segregation in intercellular spacing and grain boundaries occur. At higher magnifications, details of the precipitated second phases are also evidenced. These SEM micrographs revealed needle-like intermetallic phases and Chinese-script morphologies that could correspond to the  $\text{Al}_2\text{O}_3$ ,  $\text{Fe}_2\text{O}_3$  and  $\text{CaCO}_3$  phases respectively. In SEM analysis, the spots in white colour show presence of  $\text{CaCO}_3$  and  $\text{SiO}_2$  is shown by transparent crystals.  $\text{Al}_2\text{O}_3$  (Alumina) appearance is shown as white solid. Black colour shows the presence of hematite.

### 8.3 XRD analysis

XRD analysis was done on the selected samples to determine their surface composition. During this analysis, chemical composition of Aluminium after Thixoforming process was evaluated.

#### 8.3.1 XRD Analysis of Al-6063 alloy at temperature of 545 °C

X-ray diffraction analysis of Al-6063 alloy manufactured at temperature of 545 °C shows the presence of oxide of silicon and aluminium which are denoted as  $\text{SiO}_2$  and  $\text{Al}_2\text{O}_3$  respectively, chromium (Cr) and hematite ( $\text{Fe}_2\text{O}_3$ ). The chromium oxide can result in formation of cracks. Presence of hematite means high amount of carbon must be present in the element. Hematite crystallizes in the rhombohedral system, and it has the same crystal structure as ilmenite and corundum. Hematite is harder than pure iron, but much more brittle.

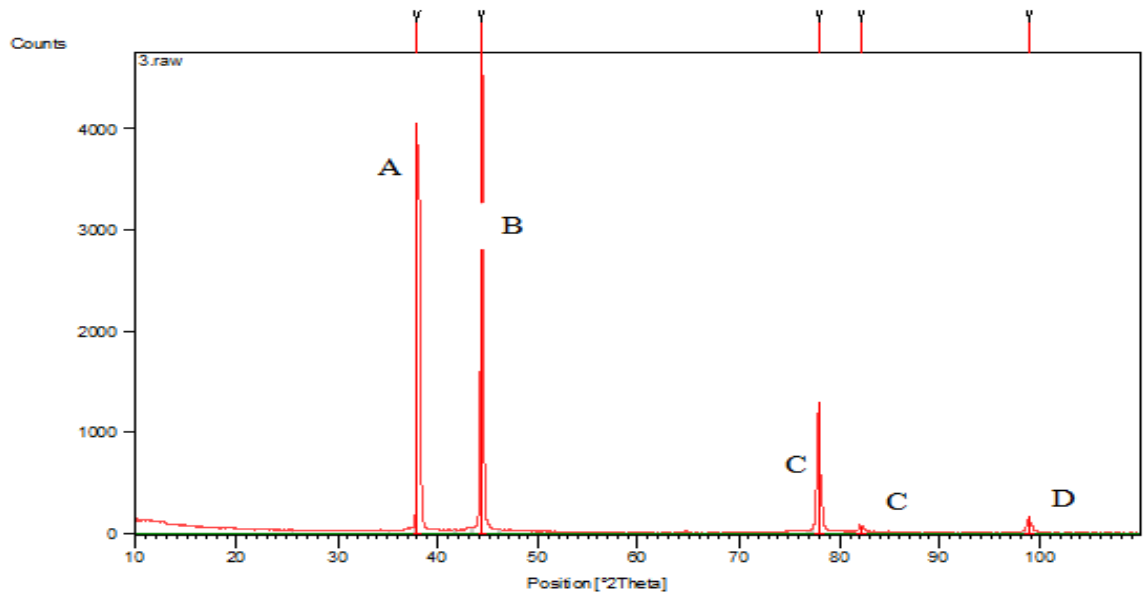


Where A-  $\text{Al}_2\text{O}_3$ , B-  $\text{SiO}_2$ , C-  $\text{Fe}_2\text{O}_3$ , D- Cr

**Fig 8.6 Al-6063 alloy at temperature 545 °C**

#### 8.3.2 XRD Analysis of Al-6063 alloy at temperature 560 °C

X-ray diffraction analysis of Al-6063 alloy manufactured at temperature of 560 °C shows the presence of oxide of silicon and aluminium which are denoted as  $\text{SiO}_2$  and  $\text{Al}_2\text{O}_3$  respectively, chromium (Cr) and hematite ( $\text{Fe}_2\text{O}_3$ ). Presence of hematite means high amount of carbon must be present in the element. Hematite crystallizes in the rhombohedral system, and it has the same crystal structure as ilmenite and corundum. Hematite is harder than pure iron, but much more brittle.

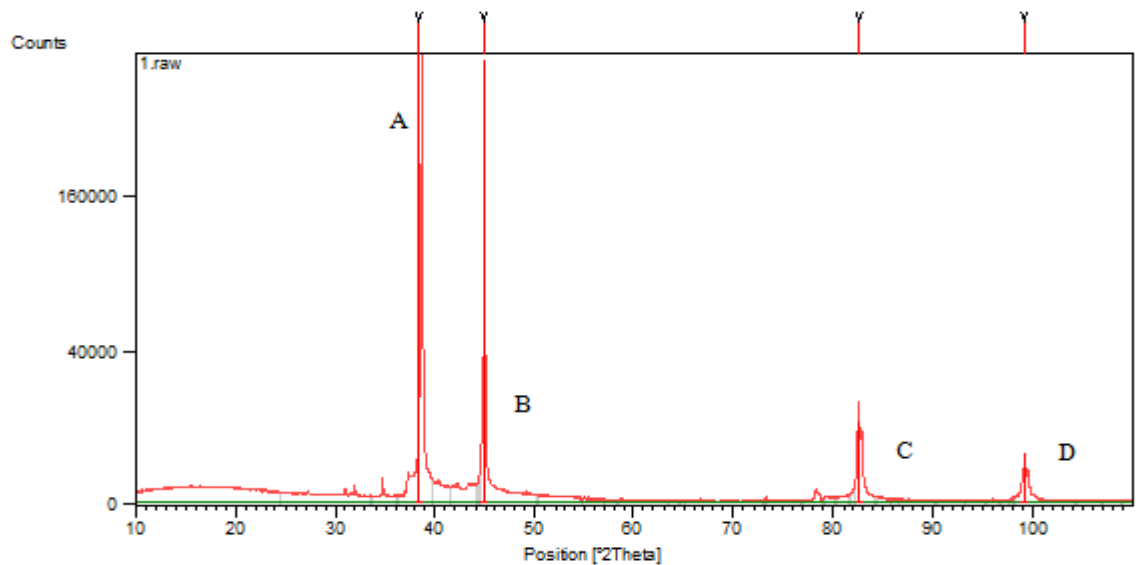


Where A-  $\text{Al}_2\text{O}_3$ , B- Cr, C-  $\text{Fe}_2\text{O}_3$ , D-  $\text{SiO}_2$

**Fig 8.7 Al-6063 alloy at temperature 560 °C**

### 8.3.3 XRD Analysis of Al-6082 alloy at temperature of 548 °C

X-ray diffraction analysis of Al-6082 alloy manufactured at temperature of 548 °C shows the presence of oxide of Aluminium which is denoted as  $\text{Al}_2\text{O}_3$ , chromium (Cr), hematite ( $\text{Fe}_2\text{O}_3$ ) and Calcium carbonate ( $\text{CaCO}_3$ ). This calcium carbonate has a large no. of applications in different industries. Its main use is in construction industry. It is white in colour and its presence has been confirmed by SEM analysis.

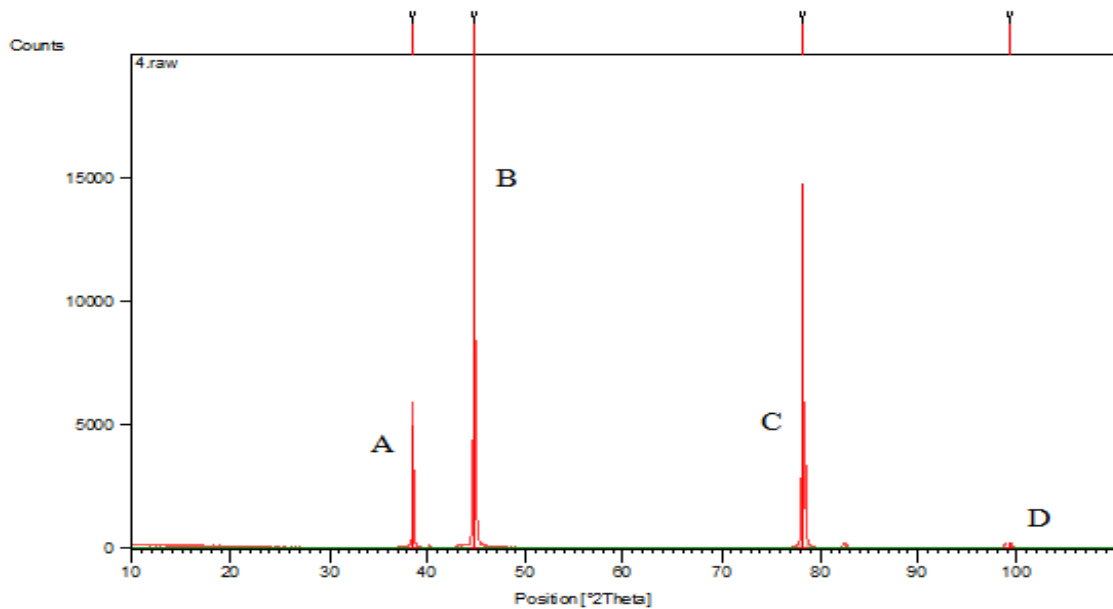


Where A-  $\text{Al}_2\text{O}_3$ , B- Cr, C-  $\text{Fe}_2\text{O}_3$ , D-  $\text{CaCO}_3$

**Fig 8.8 Al-6082 alloy at temperature of 548 °C**

### 8.3.4 XRD Analysis of Al-6082 alloy at temperature 585 °C

X-ray diffraction analysis of Al-6082 alloy manufactured at temperature of 585 °C shows the presence of oxide of silicon and aluminium which are denoted as (silicon dioxide)  $\text{SiO}_2$  and  $\text{Al}_2\text{O}_3$  respectively, hematite ( $\text{Fe}_2\text{O}_3$ ) and  $\text{Cr}_2\text{O}_3$ . Silicon dioxide or Silica is known for its hardness since ancient times. Its appearance is like transparent crystals. This oxide is formed when silicon is exposed to air or oxygen.



Where **A**-  $\text{Al}_2\text{O}_3$ , **B**-  $\text{Cr}_2\text{O}_3$ , **C**-  $\text{Fe}_2\text{O}_3$ , **D**-  $\text{SiO}_2$

**Fig 8.9 Al-6082 alloy at temperature 585 °C**

**RESULTS, CONCLUSIONS AND RECOMMENDATIONS**

**9.1 Introduction**

The effect of Thixoforming process of different Al-6 series at different temperatures was found. The mechanical property of the die got improved and the consolidated results is given below:

**9.2 Results of UTS**

**Table 9.1 Results of mechanical properties of Al-6 Series Alloy.**

S. N o.	Alloy	Temperature (°C)	Ultimate Stress (MPa)	Proof Stress (MPa)	Elongation %	BRINELL Hardness	ROCKWELL Hardness	VICKER Hardness	Reduction Area %
1	Al-6063	545	222	204	15- 16	88	9	21.536	60.62
2	Al-6063	560	245	216	16	82	8	21.580	48.86
3	Al-6082	548	394	305	15.33	110	13	26.286	46.62
4	Al-6082	585	255	233	15	87	11	22.068	36.5

**Table 9.2 Comparison the Al 6063 after Conventional Extrusion and Thixo Extrusion**

S No.	Alloy	Temperature (°C)	Ultimate Stress (MPa)	Proof Stress (MPa)	Elongation %	BRINELL Hardness (HBW)
1	6063	450	190	155	7	62
2	6063	545	222	204	15-16	88
3	6063	560	245	216	16	82

Table 9.2 shows that after Thixoforming processes the mechanical properties of Al 6063 alloy improve as comparison to conventional extrusion process. This table also show that as the temperature increase Ultimate stress, Proof stress and elongation increased.

**Table 9.3 Comparison the Al 6082 after Conventional Extrusion and Thixo Extrusion**

<b>S No.</b>	<b>Alloy</b>	<b>Temperature (°C)</b>	<b>Ultimate Stress (Mpa)</b>	<b>Proof Stress (Mpa)</b>	<b>Elongation %</b>	<b>BRINELL Hardness (HBW)</b>
1	6082	450	316	258	8	95
2	6082	548	394	305	15.33	110
3	6082	585	255	233	15	87

Table 9.3 shows that after Thixoforming process, the mechanical properties of Al 6063 alloy improves in comparison to conventional extrusion process. This table show that as the temperature increase from 450 °C to 548°C all the mechanical properties improve but when the temperature increase from 548°C to 585°C, then strength and hardness decrease but elongation is constant.

### **9.2.1 Ultimate and Proof Stress**

From Table 6.3 to 6.6, it was observed that the ultimate strength of Al-6063 alloy was increased as the temperature rises from 545 to 560 °C. The proof strength varies proportionally with temperature. But the ultimate stress of Aluminium 6082 alloy is decreased as the temperature rises from 548 to 585 °C and proof stress is decreased.

### **9.2.2 Elongation of Material**

From Table 6.3 to 6.6 it was observed that the elongation of the material is improved and it ranges from 15 to 16 % of both the Aluminium alloy (Al-6063, Al-6082).

### **9.2.3 Reduction in Area**

From Table 6.3 to 6.6 it is observed that the reduction in area of both the material is improved.

## **9.3 Result of Hardness**

It is observed that Hardness of Al-6063 and Al-6082 is improved as comparison to conventional extrusion process.

### **9.3.1 Rockwell Hardness**

From Table 7.1, it is observed that Rockwell Hardness of Al-6063 at 545°C is 9 HRC and at 560 °C is 8 HRC. So with the increase in temperature the Rockwell Hardness decreases.

From Table 7.2, it is observed that Rockwell Hardness of Al-6082 at 548°C is 13 HRC and at 585 °C is 11 HRC. So with the increase in temperature the Rockwell Hardness decreases.

### **9.3.2 Brinell Hardness**

From Table 7.3, it is observed that Brinell Hardness of Al-6063 at 545°C is 88 HBW and at 560°C is 82 HBW. So with the increase in temperature the Rockwell Hardness decreases.

From Table 7.4, it is observed that Brinell Hardness of Al-6082 at 548°C is 110 HBW and at 585°C is 87 HBW. So with the increase in temperature the Rockwell Hardness decreases.

### **9.3.3 Micro Hardness**

From Table 7.5, it is observed that Micro Hardness of Al-6063 at 545°C is 21.536 VH and at 560°C is 21.580 VH.

From Table 7.6, it is observed that Micro Hardness of Al-6082 at 548°C is 26.286 VH and at 585°C is 22.0684 VH.

## **9.4 Conclusions**

Following conclusions has been generated in the present study:

- a) Ultimate Strength of Thixoforming specimen is stable for Al-6 Series alloys in comparison with initial Hot Extrusion ones under T6 tempering condition.
- b) The yield strength of Thixoextrusion specimen is comparable with initial hot extrusion ones for Al-6 Series alloy under T6 tempering condition.
- c) It is found that the most significant factor which improves the mechanical property of the material is Ultimate Strength followed by Elongation and Hardness.
- d) During Thixoforming Process, the materials shows thixotropic behaviour as it is in semi-solid state (Containing 30-40 % liquid and 60-70 % solid). Due to this behaviour the extrusion of the material become easier.
- e) Thixotropic behaviour shows an increase in die life.

## **9.5 Recommendation for Future Work**

1. The same experiment can be performed on different temperatures and comparative results can be evaluated to find optimum conditions.
2. In the present study, only Al-6 Series alloy was taken into consideration. This type of experimentation can be done of different alloys of Aluminium.
3. Materials other than aluminium can be used for Thixoforming process.

## REFERENCES

- 1] Dey S., Basumallick A. & Chattoraj (2010), "The effect of pitting on fatigue lives of peak aged and overaged 7075 Al alloy", Vol. 41, pp. 32-41.
- [2] Xue Y., McDowell D., Hostemeyer M., Dale M., Jordon J (2007), "Microstructure based multistage fatigue modeling of Al alloy 7075-T651", Vol. 74, pp.1-6
- [3] Yang Y., Zheng H., Shi Z.G., Zhang Q (2011), "Effect of orientation on self organization of shear bands in 7075 Al alloy", Vol. 42, pp. 1462-1473.
- [4] Yang Y., LI D.H, Zhang H.G., LI X.M., Jiang F (2009), "Self organization behavior of shear bands in 7075 T73 annealed Al alloy", Vol.211, pp. 16-23.
- [5] Chayong S., Atkinson Kapranos H.P., (2005), "Thixoforming 7075 Al alloy", Vol. 528, pp. 3-12.
- [6] Vaneetveld G., Rassil D., Pierret J., Lecomte J., Beckers, (2008), "Extrusion test of 7075 Al alloy at high solid fraction", Vol. 527, pp. 1160 -1180.
- [7] Atkinson H., Burke K, Vaneetveld G. (2008), "Recrystallisation in the semi solid state in 7075 Al alloy", Vol. 9, pp. 93-105.
- [8] Rogal L., Dutkiewicz J., Goral A., Oszowska-Sobieraj B., Danko J. (2010), "Characterization of the after thixoforming microstructure of a 705 a alloy gear", Vol. 390, pp. 250-259.
- [9] Dong J., Cui J., LF Q.C., LU G. (2003), "Liquid semi continuous casting reheating and thixoforming of a wrought Al alloy 7075", Vol. 70, 43-59.
- [10] Paulodavim J., Maranhiao C., Ackson M., Cabral G., Gracio J. (2012), "FEM Analysis in high speed machining of Al a7075 alloy using polycrystalline diamond(PCD) and cemented carbide (K10) cutting tool", Vol. 490. pp.61-75.

- [11]. Rogal L., Dutkiewicz J., Goral A., Olszowska-Sobieraj B., Danko J. (2010), "Characterization of the after thixoforming microstructure of a 7075 Al alloy gear", Vol. 3, pp. 199-230.
- [12]. Dong J., Cui J., Le Q., Lu G., (2003), "Liquids semi continuous casting reheating and thixoforming of a wrought Al alloy 7075", Vol. 345, pp. 27-46.
- [13] Rikhtegar F., Ketabchi M., (2010), "Investigation of mechanical properties of 7075 Al alloy formed by forward thixoextrusion process", Vol. 31, pp. 3943-3948.
- [14] Paulo J., Davim, Maranhao C., Jackson M., Cabra C., Gracio J. (2008), "FEM Analysis in high speed machining of aluminium alloy (AL7075-0) using polycrystalline diamond (PCD) and cemented carbide (K10) cutting tools", Vol. 71, pp. 134-139.
- [15] Yang Y., Li X., Xu C., Zhang L. (2012), "Effect Of Two Different Dynamic Loading Condition On Spall And Damage Of 7075 Al Alloy", Vol. 21, pp. 624- 634.
- [16] Kilickap E. (2010), "Modelling And Optimization Of Burr Height In Drilling Of Al 7075 Using Taguchi Method And Response Surface Methodology", Vol. 49, pp. 22-28.
- [17] Zare S., Chavoshi. (2011), "Tool flank wear prediction in cnc turning of 7075 Al alloy SiC composite", Vol. 5, pp. 41 -46.
- [18] Shen J., Liu R., Liu Y., Z Jiang Z. (1997), "Microstructure and tensile properties of spray deposited high strength Al alloys", Vol. 32, pp. 229-236.
- [19] Anderson N., Leacock A., McMurray R., Brown D. (2009), "The evolution of yielding in 7075 O Al alloy: Experimental observations and modeling", Vol. 2, pp. 79-88.
- [20] Lee D., Park J., Cho D. (1997), "high temperature properties of dispersion strengthened 7075 T6 Al alloy", Vol. 16, pp. 576- 583.
- [21] Zhang K., Chen G. (2000), "Influence of SiC particulates on Grain structure development of an Al 7075 alloy during laser rapid solidification", Vol. 19, pp. 744-749.

- [22] Kumar S., Panigrahi, Jayaganthan R.(2008), “tube spin ability of AA 2024 and 7075 Al alloy” Vol. 80, pp. 66-71.
- [23] Nikanorov S., Volkov M., Gurin V., Burenkov Y.(2011), “Effect of annealing of thermal stability precipitate evolution and mechanical properties of CRYOROLLED Al 7075 Alloy”, Vol. 42, pp. 856-863.
- [24] Nikanorov S., Volkov M., Gurin V., Burenkov Y.( 2005), “Structural mechanical properties of Al-Si alloys obtained by fast cooling of a levitated melt”, Vol. 390, pp. 426-436.
- [25] Amoush A.(2007), “Investigation of corrosion behaviour of hydrogenated 7075 T6 Al alloy”, Vol. pp. 443, 3535-3550.
- [26] Ou B., Yang J. & Wei M.(2007), “Effect of homogenization and aging treatment on mechanical properties and stress corrosion cracking of 7075 alloy”, Vol. 38, pp.979-984.
- [27] Nishida Y., Sigematsu I., Arima H., Kim J., Ando T.(2002), “Super plasticity of a SiC whisker reinforced 7075 composite processed by rotary die equal channel angular pressing”, Vol. 21, pp.564-571.
- [28] Dai W.(2003), “Effect of high intensity ultrasonic wave emission on the weldability of Al alloy 7075 T6”, Vol.17, pp. 92-99.
- [29] Unlu B.(2008), “Investigation of tribological and mechanical properties Al<sub>2</sub>O<sub>3</sub>-SiC reinforce Al composites manufactured by casting or P/M Method”, Vol. 57, pp. 7-10.
- [30] Yong L., Hwan L., Seon L.(2001), “Characterization of 7075Al alloy after cold working and heating in the semi solid temperature range”, Vol. 3, pp.1-10.
- [31] Hidalgo P., Cepeda-Gimenez C., Ruano O., Carreno F.(2010), “Influence of the processing temperature on the microstructure, texture, and hardness of the 7075 Al alloy fabricated by accumulative roll bonding”, Vol. 1, pp. 394-397.
- [32] Onoro J. & Ranninger C.(1999), “stress corrosion cracking behaviour of heat treated Al-zn-mg-cu alloy with temperature”, Vol. 29, pp. 570-573.

- [33] Horita Z., Fujinami T., Minorunemoto.(2010),”Equal channel angular pressing commercial Al alloy: grain refinement, thermal stability and tensile strength”, Vol. 111, pp.1087-1098.
- [34] Adriananeag, Favier V., Vigot R.(2012),”Microstructure and flow behaviour during backward extrusion of semi solid 7075 Al alloy”, Vol.41, pp.3073-3077.
- [35] Ortiz D., Abdelshehid M., Dalton R.(2007),”effect of cold working on tensile properties of 6061, 2024 and 7075 Al alloy”, Vol. 35, pp. 272-276.
- [36] Pataric A., Mihailouic M., Gulisija M.(2012),”quantitative metallographic assessment of the electromagnetic casting influence on the microstructure of 7075 Al alloy”, Vol. 31, pp. 2172-2190.
- [37].Rajan T., Sharma C. and Sharma A.(2007), “Heat treatment principles and techniques”, Vol.212, pp 326-332.
- [38] Lee S., Oh S. (2002), “Thixoforming characteristics of thermo-mechanically treated AA6061 alloy for Suspension parts of electric vehicles”, Vol. 16. pp. 19-23
- [39] Bryner T.K.(1989), “ The composite extrusion process”, Master of Science, Ohio University.
- [40] Hirt G., Kopp R.(2009), “Thixoforming Semi solid metal process”, WILEY-VCH publisher, ISBN:978-3-527-30679-4.
- [41] Nayar A.(2005) , “Testing of Metal”, Tata Mcgraw-Hill publishing company limited, ISBN 0-07-058164-9.
- [42] [http://www.bonlalum.com/extrusion\\_process.shtml](http://www.bonlalum.com/extrusion_process.shtml), 7/11/2012.
- [43] Rajan T.V., Sharma C.P., Sharma A.,(2001), “ Heat Treatment Principles and Techniques”, Prentice Hall of India Private Limited, ISBN-81-203-0716-X.